Ph.D. Dissertation of Medicine

Comprehensive clinicopathologic, molecular, and immunologic characterization of colorectal carcinomas with loss of three intestinal markers, CDX2, SATB2, and KRT20

세가지 장표지자 (CDX2, SATB2, KRT20)의 소실을 보이는 대장암의 종합적인 임상병리학적, 분자적 및 면역학적 특성에 대한 규명

February 2023

Graduate School of Medicine
Seoul National University
Pathology Major

이지애

Comprehensive clinicopathologic, molecular, and immunologic characterization of colorectal carcinomas with loss of three intestinal markers, CDX2, SATB2, and KRT20

지도 교수 강경훈

Submitting a Ph.D. Dissertation of
Medicine

October 2022

Graduate School of Medicine
Seoul National University
Pathology Major

이지애

Confirming the Ph.D. Dissertation written by
이지애
January 2023

Chair _____(Seal)
Vice Chair _____(Seal)
Examiner _____(Seal)
Examiner _____(Seal)
Examiner _____(Seal)

Abstract

Caudal-type homeobox 2 (CDX2), special AT-rich sequence-binding protein 2 (SATB2), and keratin 20 (KRT20) are frequently used as intestinal epithelium-specific markers in immunohistochemical studies. However, subsets of colorectal carcinomas (CRCs) show loss of these markers. We analyzed The Cancer Genome Atlas data to explore molecular correlates of *CDX2, SATB2*, and *KRT20* genes in 390 CRCs. The decreased mRNA expression of each of the three genes commonly correlated with microsatellite instability-high (MSI-H), CpG island methylator phenotype-high (CIMP-H), *BRAF/RNF43* mutations, consensus molecular subtype 1, and high tumor mutational burden. The downregulation of *CDX2* or *SATB2* was dependent on both MSI-H and CIMP-H, whereas that of *KRT20* was more dependent on MSI-H than on CIMP-H. Next, we evaluated the immunohistochemical expression of CDX2, SATB2, and KRT20 in 436 primary CRCs. In contrast to RNA-level expression, decreased expression of CDX2 and SATB2 was more dependent on CIMP-H than on MSI-H. However, consistent with RNA-level expression, decreased expression of KRT20 was more dependent on MSI-H than on CIMP-H. CIMP-H and lymphatic invasion were consistently associated with both CDX2 loss and SATB2 loss in CRCs, regardless of MSI status. Cases with concurrent loss of all three markers were found exclusively in *MLH1*-methylated MSI-H/CIMP-H CRCs. In conculsion, MSI-H and/or CIMP-H are major common correlates of decreased CDX2/SATB2/KRT20 expression in CRCs, but the specific features associated with the loss of each marker are different in CRCs.

Keyword : colorectal cancer, immunohistochemistry, caudal-type homeobox 2 (CDX2), special AT-rich sequence-binding protein 2, cytokeratin 20

Student number : 2017-22049

Table of Contents

Chapter 1. Introduction

1.1. Study Background

Colorectal carcinoma (CRC) is the third most common cancer in the USA, and it is estimated that approximately 150,000 individuals will be newly diagnosed with CRC in 2021 [1]. Approximately 20% of CRC patients present with distant metastasis at the time of diagnosis (stage IV) [2], and 18% of non-stage IV CRC patients that undergo curative surgery, experience metachronous metastasis (distant recurrence) within 5 years after surgery [3]. In the case of suspected metastasis of CRC or extra-colonic adenocarcinoma of unknown primary, pathologic diagnosis using immunohistochemistry (IHC) for intestinal epithelium-specific markers is important to confirm whether the colorectum is the primary site of metastatic tumors.

Caudal-type homeobox 2 (CDX2) and keratin 20 (KRT20, also known as cytokeratin 20 or CK20) are highly expressed in the lower gastrointestinal tract epithelium and have been frequently used as IHC markers for the differential diagnosis of epithelial tumors of lower gastrointestinal tract origin [4-8]. These proteins play critical roles in the normal physiologic differentiation of the intestinal epithelium [9-11]. Although their expression is maintained in most CRCs, the loss of CDX2 and/or KRT20 expression is seen in a small subset of CRCs and is associated with poor prognosis in CRC [12-17].

In addition to CDX2 and KRT20, special AT-rich sequence-binding protein 2 (SATB2) has been recently recognized as a sensitive and specific marker for CRC [18]. In particular, SATB2 IHC showed excellent specificity for CRC when used as a combined marker with KRT20 [19, 20] and can be used as a marker supplementary to CDX2 in the diagnosis of metastatic CRC [21]. Similar to CDX2 and KRT20, the loss of SATB2 expression can be observed in a small subset of CRCs and is associated with poor

survival in CRC patients [22–24]. It has been reported that loss of CDX2, SATB2, or KRT20 expression is molecularly associated with microsatellite instability–high (MSI–H) and/or CpG island methylator phenotype–high (CIMP–H) in CRCs [12, 16, 17, 22, 24–27].

1.2. Purpose of Research

An in–depth understanding of the features specific to CRCs lacking intestinal markers is critical for differential diagnosis as well as the identification of the site of tumor origin. Although the pathologic characteristics of CRCs with reduced IHC expression of intestinal markers have been studied before, there is a lack of investigations focusing on the combined genetic, epigenetic, and transcriptional basis of alterations of all three intestinal markers in CRC. Therefore, in this study, we comprehensively analyzed RNA– and protein–level alterations of the three intestinal markers, namely, CDX2, SATB2, and KRT20, and their clinicopathologic, molecular, and immunologic correlations in large samples of CRCs using The Cancer Genome Atlas (TCGA) datasets and primary CRC tissue cohorts.

Chapter 2. Body

2.1 Materials and methods

Tissue samples

Formalin-fixed paraffin-embedded (FFPE) tissues of 436 primary CRCs, including 131 MSI-H and 305 microsatellite stable (MSS) CRCs, were collected from the pathology archive of Seoul National University Hospital (SNUH), Seoul, Korea. All tissues were obtained from surgically resected specimens from CRC patients who underwent surgical treatment at SNUH between 2014 and 2018 (MSI-H cohort) or in 2018 (MSS cohort). All 436 CRC samples were identified as MSI-H or MSS by fluorescence capillary electrophoresis-based DNA fragment analysis using five Bethesda microsatellite markers (BAT-25, BAT-26, D2S123, D5S346, D17S250) [28]. A sample was defined as MSI-H when ≥ 2 microsatellite markers showed instability in tumor DNA compared with normal mucosa DNA, and as MSS when ≤ 1 marker showed instability in tumor DNA compared with normal mucosa DNA. Employing MLH1/MSH2/MSH6/PMS2 IHC, the MSI-H and MSS CRCs were confirmed to be DNA mismatch repair (MMR) deficient or proficient, respectively; the tumors that showed equivocal results in MMR IHC were excluded from the study. Germline DNA sequencing for MMR genes was not conducted. Thus, exact status of hereditary MSI-H CRCs of Lynch syndrome was unavailable.

This study was approved by the Institutional Review Board of SNUH (IRB No. 1804-036-935).

Clinicopathologic analysis

Clinical information, including age, sex, tumor location, and clinical evidence of distant metastasis (cM) or tumor recurrence, was obtained by reviewing electronic medical records of the patients from which the samples were obtained. Pathologic parameters, including gross tumor type, tumor size, depth of invasion (pT), lymph node

metastasis (pN), pathologic evidence of distant metastasis (pM) or tumor recurrence, lymphatic/venous/perineural invasion, tumor differentiation, mucinous histology, signet ring cell histology, tumor budding, poorly differentiated clusters (PDCs), desmoplastic reaction (DR), and tertiary lymphoid structure (TLS) activity, were evaluated by gastrointestinal pathologists (J.A.L. and J.H.K.) Tumor budding was graded using a three-tier system (low [BD1], intermediate [BD2], and high [BD3]) according to the criteria suggested by the International Tumor Budding Consensus Conference [29]. PDC status was classified into one of three grades (G1, G2, and G3) according to Ueno's classification [30]. DR status was histologically categorized into one of three patterns (mature, intermediate, and immature) based on the criteria suggested by Ueno et al. [31] To assess TLS activity, we used Ueno's criteria (measuring the maximum diameter of the largest TLS with a 1-mm cutoff value) as previously described [32, 33].

Immunohistochemistry

Multi-core tissue microarray (TMA) blocks of the 131 MSI-H CRCs and 305 MSS CRCs were constructed as previously described [34]. Four representative tumor areas, two of which were from the invasive margin (IM) area and two from the center of the tumor (CT) area, were selected on FFPE tissue blocks of each CRC, and TMA cores (2 mm in diameter) were extracted from each of the four areas. Therefore, each case consisted of four tumor cores. All 436 CRCs were analyzed by IHC using primary antibodies against CDX2 (Ventana ERP2764Y clone, Roche, Basel, Switzerland; RTU), SATB2 (EPNCIR130A clone, Abcam, Cambridge, UK; 1:100), KRT20 (CK20) (DAKO Ks20.8 clone, Agilent Technologies, Santa Clara, CA, USA; 1:50), KRT7 (CK7) (DAKO OV-TL 12/30 clone, Agilent Technologies; 1:300), MLH1 (Ventana M1 clone, Roche; RTU), MSH2 (Ventana G219-1129 clone, Roche; RTU), MSH6 (Cell Marque 44 clone, MilliporeSigma, Burlington, MA, USA; 1:50), PMS2 (Cell Marque MRQ-28 clone, MilliporeSigma; 1:50), CD3 (Confirm 2GV6 clone, Roche; RTU), and CD8 (Confirm SP57 clone, Roche;

RTU). IHC was performed on TMA slides (CDX2, SATB2, KRT20, KRT7, MLH1, MSH2, MSH6, and PMS2) or representative whole tumor slides (CD3 and CD8). IHC staining was performed using automated immunostainers (Ventana BenchMark XT, Roche or Bond-III, Leica Biosystems, Wetzlar, Germany).

Evaluation of CDX2, SATB2, and KRT20 IHC expression

CDX2 and SATB2 IHC positivity was determined by nuclear staining, and KRT20 IHC positivity was determined by cytoplasmic and/or membranous staining. To estimate the quantitative expression of CDX2, SATB2, and KRT20 IHC in the CRCs, we determined their H-scores because it reflects the quantitative characteristics of IHC expression in tissue sections based on staining intensity(0: negative/1+: weak positive/2+: moderately positive/3+: strong positive) and the proportion (%) of positive (stained) cells. The H-score of CDX2, SATB2, or KRT20 was calculated using the following formula: [1 × (percentage of 1+ cells in tumor area) + 2 × (percentage of 2+ cells in tumor area) + 3 × (percentage of 3+ cells in tumor area)] [35].

Tumor-infiltrating lymphocytes (TIL) immunoscore

TIL in CRC tissues were quantified as previously described [34]. Briefly, CD3/CD8 IHC slides were scanned as digital images using an Aperio AT2 slide scanner (Leica Biosystems) at 20x magnification with a resolution of 0.5 μm per pixel. Enumeration of TIL was performed using the 'positive cell detection' program of the QuPath software, a validated open source software for digital pathology image anlysis [36, 37]. The density of CD3+ or CD8+ TIL at the IM or CT area was defined as the number of positive cells per IM or CT field area (cells/mm2) [34]. The TIL immunoscore was calculated using four TIL parameters, including CD3+ TIL density at the IM, CD3+ TIL density at the CT, CD8+ TIL density at the IM, and CD8+ TIL density at the CT, according to Galon's critera [38,39].

Analysis of CIMP and *KRAS/BRAF* mutations

DNA analyses for determining CIMP and *KRAS/BRAF* mutations were performed using tumor DNA samples from the 131 MSI-H CRCs and 305 MSS CRCs, as previously described [40]. Briefly, CIMP status was analyzed by methylation-specific real-time PCR (MethyLight assay) using eight CIMP-specific promoter markers (*MLH1, CDKN2A (p16), NEUROG1, CACNA1G, CRABP1, IGF2, RUNX3,* and *SOCS1*). A tumor sample was classified as CIMP-H when it showed CpG island hypermethylation in five or more markers. Mutations in *KRAS* exons 2, 3, and 4 and *BRAF* exon 15 were double-tested by Sanger sequencing and peptide nucleic acid (PNA) clamping-mediated real-time PCR using the PNAClamp Mutation Detection Kit (Panagene, Daejeon, South Korea).

TCGA data analysis

Data of genomic variants, RNA expression, MSI and CIMP from 390 CRC samples were collected from publicly available TCGA-COAD and TCGA-READ datasets. RNA sequencing data was downloaded from https://gdc.cancer.gov/about-data/publications/pancanatlas, it was log2-transformed using the RSEM algorithm, and the log2-transformed RSEM expression values were used for RNA expression analysis. The ggdensity function of the ggpubr R package was used to identify the distribution of mRNA expression values of the three intestinal marker genes (CDX2, SATB2, and KRT20). For analyzing the tumor mutational burden (TMB) and specific genetic mutations the MC3 MAF file from https://gdc.cancer.gov/about-data/publications/mc3-2017 was used. Only non-synonymous variants were included for calculating the TMB, and TMB was expressed as the number of non-synonymous mutations per megabase. Mutations in 11 genes that are known to be major oncogenic drivers in CRCs, including *APC, TP53 KRAS, NRAS, BRAF, FBXW7, PIK3CA, PTEN, SMAD4, CTNNB1*, and *RNF43* mutations, were selected for further analysis. To identify oncogenic mutations in these genes, pathogenic or likely pathogenic variants reported in knowledge bases such as ClinVar

(https://www.ncbi.nlm.nih.gov/clinvar), COSMIC (https://cancer.sanger.ac.uk/cosmic), OncoKB (https://www.oncokb.org), and Cancer Hotspots (https://www.cancerhotspots.org) were included, but variants reported as single nucleotide polymorphism in dbSNP (https://www.ncbi.nlm.nih.gov/snp) were excluded from our analysis. Consensus molecular subtype (CMS) data provided by the Colorectal Cancer Subtyping Consortium were also used [41]. Based on the expression levels of each of the three intestinal marker genes (CDX2, SATB2, and KRT20), the 390 TCGA CRCs were classified into the following three intestinal gene expression subgroups: high (higher than the 75th percentile), intermediate (between 25th and 75th percentile), and low (lower than 25th percentile). To identify the molecular factors associated with decreased expression of intestinal marker genes in CRC, the determined molecular features, including MSI, CIMP, CMS, TMB, and mutations in *APC, TP53, KRAS, NRAS, BRAF, FBXW7, PIK3CA, PTEN, SMAD4, CTNNB1,* and *RNF43*, were comprehensively compared between the intestinal gene expression-high/intermediate and expression-low subgroups.

Statistical analysis

Statistical analyses in this study were performed using GraphPad Prism (version 9.0.0; GraphPad Software, San Diego, CA, USA) or R version 4.0.2 (The R Foundation for Statistical Computing, www.R-project.org). The categorical variables between sample subgroups were compared using the chi-square test or Fisher's exact test. The continuous variables between sample subgroups were compared using Student's t-test or Mann-Whitney U test. Correlations between gene expression values were analyzed using Spearman's rank correlation coefficient test. All p-values were two-sided, and statistical significance was set at $p < 0.05$.

2.2 Results

Molecular correlates of RNA-level expression alterations of intestinal markers in CRCs

We first investigated the relationship between the three intestinal marker genes, namely *CDX2, SATB2,* and *KRT20* using RNA-sequencing data from TCGA CRCs (n=390 from TCGA-COAD and TCGA-READ datasets). We found significant positive correlations between mRNA expression levels of *CDX2* and *SATB2, CDX2* and *KRT20*, and *SATB2* and *KRT20* (Fig. 1a), and the correlation between *CDX2* and *SATB2* was the most significant ($r = 0.53$, $p < 0.0001$; Fig. 1a).

Because the loss of expression of intestinal markers has been associated with MSI and/or CIMP status in CRCs, we compared the distribution patterns of mRNA expression levels of the three intestinal marker genes between MSI-H and MSS subgroup (Fig. 1b), as well as in the CIMP-H than in the CIMP-L/0 subgroup (Fig. 1c). Interestingly, the distribution patterns of mRNA expression were quite similar between the MSI-H and CIMP-H subgroups (Fig. 1b, c).

To better understand the impact of CIMP and MSI on the expression of intestinal marker genes in CRC, we classified TCGA CRCs into four subgroups based on combine MSI and CIMP status (MSI-H/CIMP-H, MSS/CIMP-H, MSI-H/CIMP-L/0, and MSS/CIMP-L/0). We found that *CDX2* and *SATB2* mRNA expression levels were decreased in the subgroups with either MSI-H or CIMP-H than in the MSS/CIMP-L/0 subgroup, whereas there were no significant differences in gene expression between the three subgroups with either MSI-H or CIMP-H (Fig. 1d). In contrast, KRT20 expression levels were significantly lower in the MSI-H subgroups (MSI-H/CIMP-H and MSI-H/CIMP-L/0) than in the MSS subgroups (MSS/CIMP-H and MSS/CIMP-L/0) regardless of CIMP status (Fig. 1d).

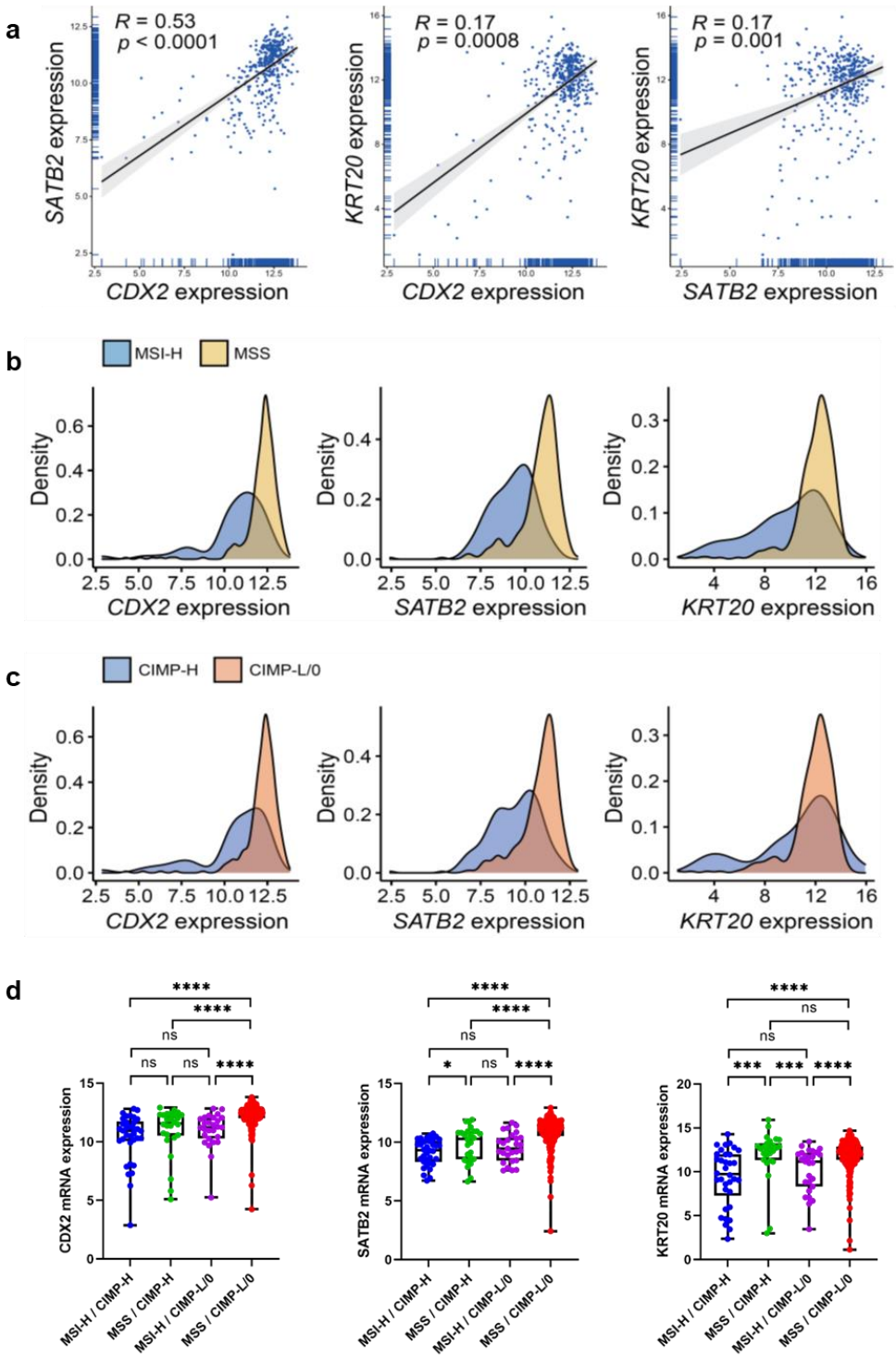

Fig 1. Decreased mRNA expression of intestinal marker genes is associated with CIMP and MSI status in TCGA CRCs (n=390). **a** Correlation scatter plots displaying the mRNA expression levels of three intestinal marker

genes (*CDX2, SATB2, and KRT20*) in TCGA CRCs. **b** Distribution of mRNA expression levels of *CDX2, SATB2,* and *KRT20* in MSI−H and MSS subgroups of TCGA CRCs. **c** Distribution of mRNA expression levels of *CDX2, SATB2*, and *KRT20* in CIMP−H and CIMP−L/0 subgroups of TCGA CRCs. **d** comparison of mRNA expression levels of *CDX2, SATB2,* and *KRT20* between four combined MSI/CIMP subgroups of TCGA CRCs (MSI−H/CIMPH, MSS/CIMP−H, MSI−H/CIMP−L/0, and MSS/CIMP−L/0) (****,$p < 0.0001$; ***, $p < 0.001$; **, $p < 0.01$; *, $p < 0.05$; ns, not significant)

Next, to explore the major genomic alterations associated with the decreased expression of intestinal marker genes in CRC, TCGA CRCs were categorized into three subgroups, based on mRNA expression levels of each intestinal marker gene, as low, intermediate, and high, and major molecular factors were compared between the intestinal marker gene expression−low subgroup and the intestinal marker gene expression−high/intermediate subgroup. We found that MSI−H, CIMP−H, CMS1, *BRAF* mutation, APC wild−type, RNAF43 mutation, and high TMB were commonly more enriched in the intestinal marker gene−low subgroups of TCGA CRCs (Fig. 2a-c).

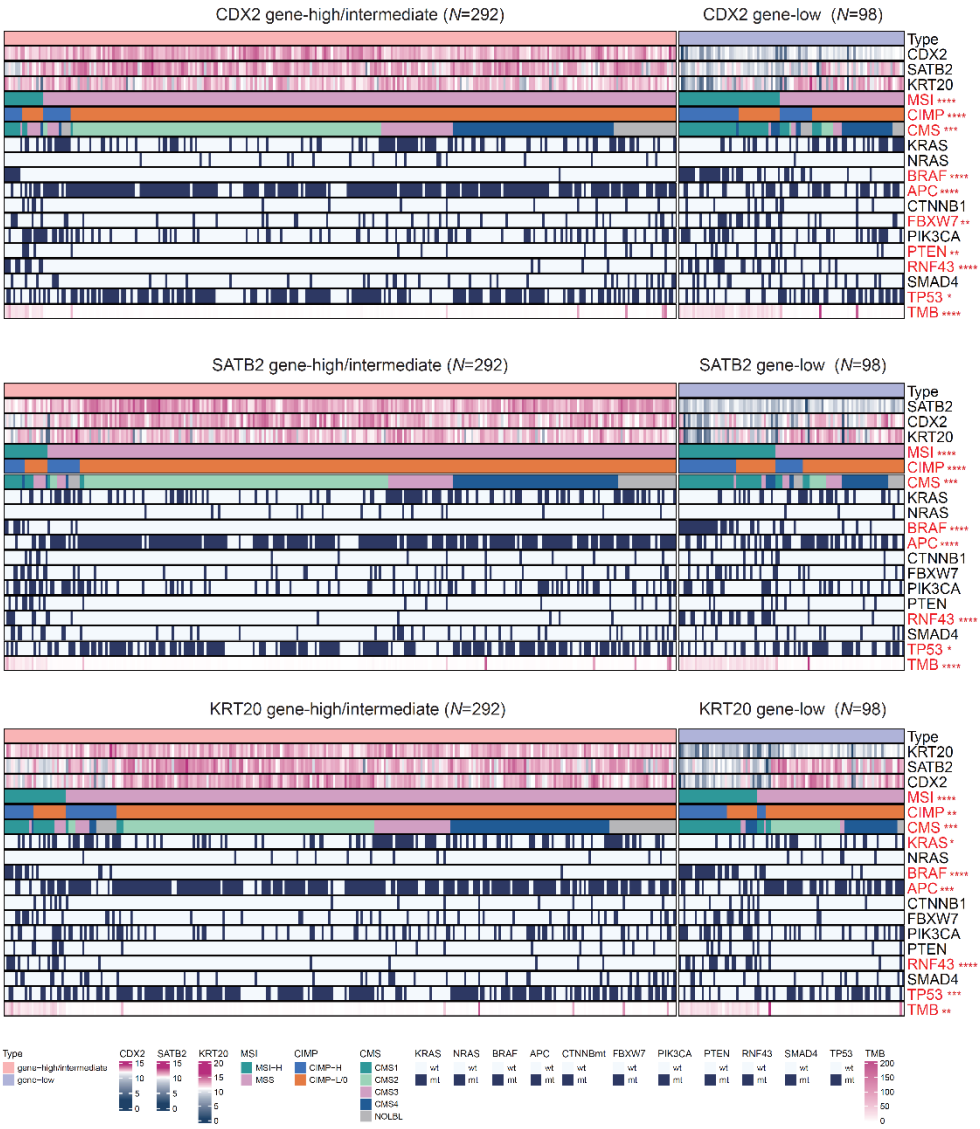

Fig 2. Molecular landscape of TCGA CRCs according to intestinal marker gene expression status. **a** Comparison of major genetic and epigenetic factors between CDX2 expression-high/intermediate and CDX2 expression-low subgroups of TCGA CRCs. **b** Comparison of major genetic and epigenetic factors between *SATB2* expression-high/intermediate and *SATB2* expression-low subgroups of TCGA CRCs. **c** Comparison of major genetic and epigenetic factors between *KRT20* expression-high/intermediate and *KRT20* expression-low subgroups of TCGA CRCs (red font denotes molecular factors that are significantly different between the intestinal marker gene-high/intermediate and intestinal marker gene-low subgroups (****, $p < 0.0001$; ***, $p < 0.001$; **, $p < 0.01$; *, $p < 0.05$)

Association of protein-level expression alterations of intestinal markers with MSI/CIMP status in CRCs

We analyzed the IHC expression of CDX2, SATB2, and KRT20 in 436 primary CRC tissues, including 305 MSS and 131 MSI-H CRCs. The relative frequency distribution patterns of H-scores of each intestinal marker IHC (Fig. 3a, b) reveal that the protein-level landscape in CRCs is similar to the pattern of RNA-level expression in TCGA CRCs (Fig. 1b, c). We found decreased IHC expression (lower H-scores) of each intestinal marker in MSI-H CRCs than in MSS CRCs (Fig. 3a), and in CIMP-H CRCs than in CIMP-L/0 CRCs (Fig. 3b).

The 436 CRCs were classified into four subgroups based on combined MSI and CIMP status (MSI-H/CIMP-H, MSS/CIMP-H, MSI-H/CIMP-L/0, and MSS/CIMP-L/0). Contrary to mRNA expression (Fig. 1d), CDX2 and SATB2 IHC expression levels were significantly lower in the CIMP-H subgroups (MSI-H/CIMP-H and MSS/CIMP-H) than in the CIMP-L/0 subgroups (MSI-H/CIMP-L/0 and MSS/CIMP-L/0) in CRC regardless of MSI status (Fig. 3c). In contrast, KRT20 IHC expression levels were significantly lower in the MSI-H/CIMP-H and MSI-H/CIMP-L/0 subgroups than in the MSS/CIMP-H and MSS/CIMP-L/0 subgroups (Fig. 3c), suggesting that the protein-level expression alteration of KRT20 may be more dependent on MSI than on CIMP status in CRCs.

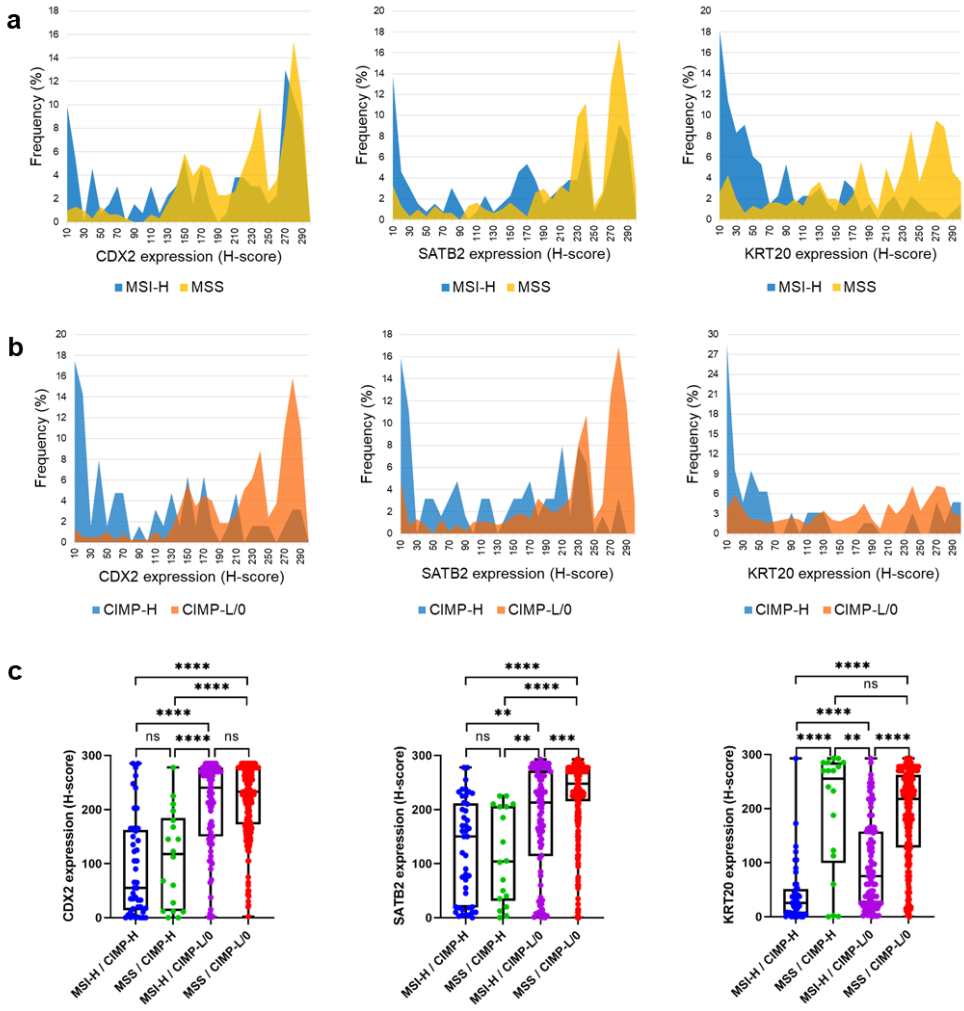

Fig. 3 Decreased expression of intestinal marker proteins is associated with CIMP and MSI status in primary CRC tissues (n=436). **a** Distribution of H-scores of CDX2, SATB2, and KRT20 IHC expression in MSI-H and MSS CRCs. **b** Distribution of H-scores of CDX2, SATB2, and KRT20 IHC expression in CIMP-H and CIMP-L/0 CRCs. **c** Comparison of IHC expression levels of CDX2, SATB2, and KRT20 between four combined MSI/CIMP subgroups of CRCs (MSI-H/CIMP-H, MSS/CIMP-H, MSI-H/CIMP-L/0, and MSS/CIMP-L/0). (****, $p < 0.0001$; ***, $p < 0.001$; **, $p < 0.01$; *, $p < 0.05$; ns, not significant)

Clinicopathologic, molecular, and immunologic features associated with the loss of intestinal marker expression in CRCs

We defined the loss of each intestinal maker IHC expression in CRC tissues as an H-score<20 based on the following features: (1) H-scores of intestinal markers commonly showed bimodal distributions (Fig. 3a, b), and cases showing low-level expression of each intestinal marker in MSI-H and CIMP-H CRCs were commonly concentrated in the H-score < 20 area (Fig. 3a, b). (2) An H-score < 20 also represents the loss of normally distinguishable (2+) staining pattern in most of the tumor area (>90%). The proportion of cases showing loss of each intestinal marker expression in MSS and MSI-H CRCs is depicted in Fig. 4a. We found that CRCs with a loss of expression of at least one of the
three intestinal markers were more enriched in MSI-H CRCs (57 of 131; 43.5%) than in MSS CRCs (38 of 305; 12.5%) (Fig. 4a). Interestingly, tumors showing loss of expression of all three intestinal markers (CDX2-/SATB2-/KRT20-) were found only in MSI-H CRCs (Fig. 4a).

Clinicopathologic, molecular, and immunologic features of CRCs with the loss of intestinal marker expression were evaluated separately in the MSS and MSI-H CRCs to minimize potential confounding effects of MSI-dependent characteristics (Fig. 4 and Tables 1-6). In both MSS and MSI-H CRCs, CDX2 loss was significantly associated with lymphatic invasion ($p = 0.001$ for MSS; $p = 0.002$ for MSI-H), tumor budding-high ($p = 0.012$ for MSS; $p = 0.014$ for MSI-H), poor differentiation ($p < 0.001$ for MSS; $p = 0.003$ for MSI-H), and CIMP-H status ($p < 0.001$ for MSS and MSI-H) (Fig. 4b and Tables1-2). Similar to CDX2 loss, SATB2 loss was correlated with lymphatic invasion ($p = 0.001$ for MSS; $p = 0.005$ for MSI-H) and CIMP-H status ($p = 0.006$ for MSS; $p = 0.024$ for MSI-H) in both MSS and MSI-H CRCs (Fig. 4b and Tables 3, 4). Interestingly, SATB2 loss was significantly associated with KRAS mutations ($p = 0.004$) and a low TIL immunoscore ($p = 0.015$) only in MSS CRCs and not in MSI-H CRCs (Fig. 4b and Tables 3, 4). Tumors with the lowest immunoscore (I0) were predominant in

SATB2−loss MSS CRCs (57%) than in SATB2−positive MSS CRCs (21%) (Fig. 4c). The density of CD8 + TIL at the IM area of SATB2−loss MSS CRCs was significantly lower than that of SATB2−positive MSS CRCs ($p = 0.006$) (Fig. 4c). KRT20 loss was significantly associated with poor differentiation in both MSS and MSI−H CRCs ($p = 0.009$ for MSS; $p = 0.023$ for MSI−H) (Fig. 4b and Tables 5, 6). Interestingly, KRT20 loss was significantly correlated with CDX2 loss only in MSI−H CRCs and not in MSS CRCs ($p < 0.001$ for MSI−H; $p = 0.396$ for MSS) (Fig. 4b).

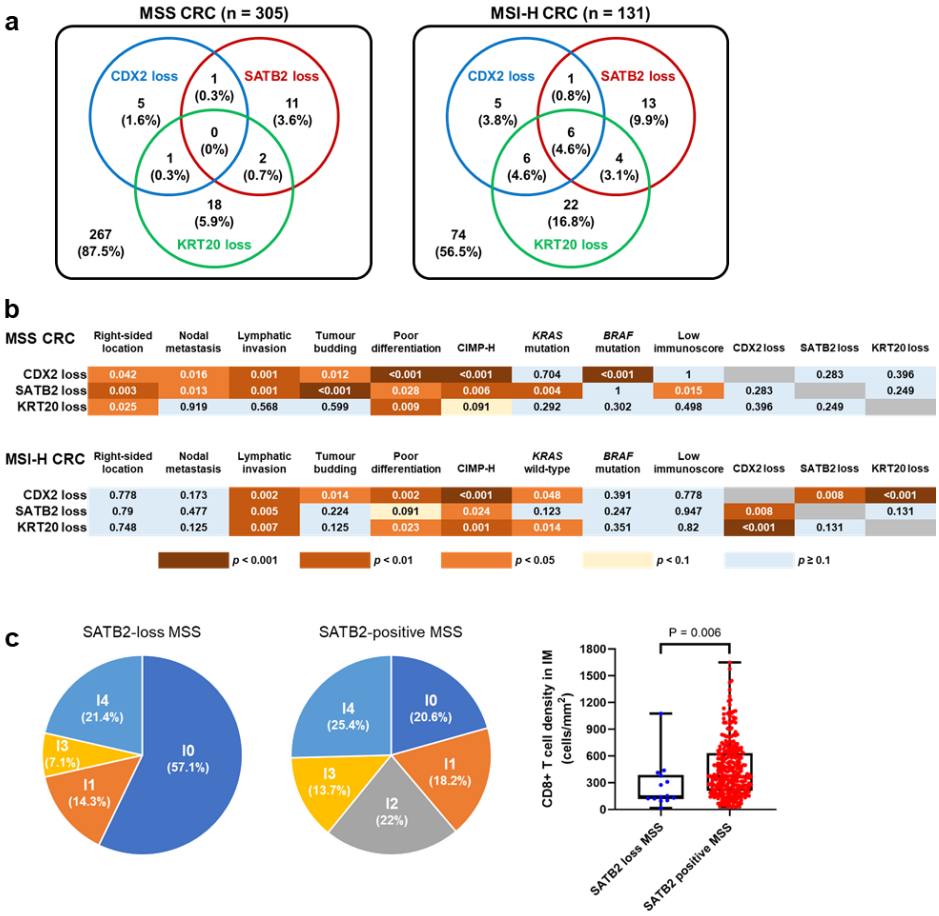

Fig. 4 Clinicopathologic, molecular, and immunologic features of CRCs with loss of intestinal marker expression. **a** Venn diagrams of the frequencies of MSS and MSI-H CRCs showing loss of intestinal marker expression. Note the presence of cases showing concurrent loss of all the three intestinal markers in MSI-H CRCs. **b** Graphical summary of the correlations between the loss of each intestinal marker and major clinicopathologic and molecular factors in MSS and MSI-H CRCs. **c** Associations between SATB2 expression status and tumor immunity in MSS CRCs Comparison of proportions of TIL immunoscores (I0-I4) between SATB2-loss and SATB2-positive MSS CRCs (left, pie charts). CD8 + TIL density at the IM area is significantly lower in SATB2-loss MSS CRCs than in SATB2-positive MSS CRCs (right, box-whisker plot)

Table 1. Differential clinicopathologic, molecular, and immunologic characteristics of MSS CRCs according to CDX2 IHC expression status (n = 305)

Variable		CDX2 loss (n = 7)	CDX2 positive (n = 298)	*p*-value
Clinicopathologic factors				
Age	Older (≥ 65 years)	3 (42.9%)	161 (54.0%)	0.708
	Younger (< 65 years)	4 (57.1%)	137 (46.0%)	
Sex	Male	3 (42.9%)	174 (58.4%)	0.459
	Female	4 (57.1%)	124 (41.6%)	
Tumor location	Right-sided colon	4 (57.1%)	62 (20.8%)	0.042
	Left-sided colorectum	3 (42.9%)	236 (79.2%)	
Gross tumor type	Polypoid or fungating	0 (0.0%)	126 (42.3%)	0.044
	Ulceroinfiltrative	7 (100.0%)	172 (57.7%)	
Tumor size	Larger (≥ 5.0 cm)	5 (71.4%)	148 (49.7%)	0.448
	Smaller (< 5.0 cm)	2 (28.6%)	150 (50.3%)	
AJCC/UICC cancer stage	Stage I/II	0 (0.0%)	134 (45.0%)	0.019
	Stage III/IV	7 (100.0%)	164 (55.0%)	
Depth of invasion (pT)	Submucosa or proper muscle (pT1/pT2)	0 (0.0%)	46 (15.4%)	0.600
	Beyond the proper muscle (pT3/pT4)	7 (100.0%)	252 (84.6%)	
Lymph node metastasis (pN)	Absent (pN0)	0 (0%)	142 (47.7%)	0.016
	Present (pN1/pN2)	7 (100%)	156 (52.3%)	
Distant metastasis (pM or cM)	Absent (M0)	4 (57.1%)	241 (80.9%)	0.140
	Present (M1)	5 (42.9%)	57 (19.1%)	
Early recurrence[a]	Absent	6 (85.7%)	267 (89.9%)	0.533
	Present	1 (14.3%)	30 (10.1%)	
Lymphatic invasion	Absent	0 (0%)	192 (64.4%)	0.001
	Present	7 (100%)	106 (35.6%)	

Venous invasion	Absent	5 (71.4%)	231 (77.5%)	0.658
	Present	2 (28.6%)	67 (22.5%)	
Perineural invasion	Absent	0 (0.0%)	135 (45.3%)	0.019
	Present	7 (100.0%)	163 (54.7%)	
Tumor differentiation	Well to moderately differentiated	1 (14.3%)	283 (95%)	< 0.001
	Poorly differentiated	6 (85.7%)	15 (5%)	
Mucinous histology	Non-mucinous (< 50%)	7 (100.0%)	288 (96.6%)	1.000
	Mucinous (≥ 50%)	0 (0.0%)	10 (3.4%)	
Signet ring cell histology	Absent	7 (100.0%)	291 (98.0%)	1.000
	Present (≥ 5%)	0 (0.0%)	6 (2.0%)	
Tumor budding	Low or intermediate	1 (14.3%)	189 (63.6%)	0.012
	High	6 (85.7%)	108 (36.4%)	
Poorly differentiated clusters	G1 or G2	1 (14.3%)	137 (46.1%)	0.132
	G3	6 (85.7%)	160 (53.9%)	
Desmoplastic reaction	Mature or intermediate	7 (100.0%)	263 (88.6%)	1.000
	Immature	0 (0.0%)	34 (11.44%)	
Molecular factors				
CIMP	CIMP-H	5 (71.4%)	13 (4.4%)	< 0.001
	CIMP-L/0	2 (28.6%)	285 (95.6%)	
MLH1 promoter methylation	Methylated	0 (0.0%)	3 (1.0%)	1.000
	Unmethylated	7 (100.0%)	295 (99.0%)	
CACNA1G promoter methylation	Methylated	5 (71.4%)	18 (6.0%)	<0.001
	Unmethylated	2 (28.6%)	280 (94.0%)	
SOCS1 promoter methylation	Methylated	1 (14.3%)	7 (2.3%)	0.171
	Unmethylated	6 (85.7%)	291 (97.7%)	
CRABP1 promoter methylation	Methylated	6 (85.7%)	66 (22.1%)	0.001
	Unmethylated	1 (14.3%)	232 (77.9%)	

RUNX3 promoter methylation	Methylated	4 (57.1%)	17 (5.7%)	0.001
	Unmethylated	3 (42.9%)	281 (94.3%)	
IGF2 promoter methylation	Methylated	5 (71.4%)	20 (6.7%)	<0.001
	Unmethylated	2 (28.6%)	278 (93.3%)	
CDKN2A promoter methylation	Methylated	5 (71.4%)	48 (16.1%)	0.002
	Unmethylated	2 (28.6%)	250 (83.9%)	
NEUROG1 promoter methylation	Methylated	5 (71.4%)	66 (22.1%)	0.009
	Unmethylated	2 (28.6%)	232 (77.9%)	
KRAS mutation[b]	Absent	5 (71.4%)	173 (58.2%)	0.704
	Present	2 (28.6%)	124 (41.8%)	
BRAF mutation	Absent	3 (42.9%)	297 (99.7%)	< 0.001
	Present	4 (57.1%)	1 (0.3%)	
SATB2 expression	Loss	1 (14.3%)	13 (4.4%)	0.283
	Positive	6 (85.7%)	285 (95.6%)	
KRT20 expression	Loss	1 (14.3%)	20 (6.7%)	0.396
	Positive	6 (85.7%)	278 (93.3%)	
Immunologic factors				
TIL immunoscore	Intermediate to high (IS-2/3/4)	4 (57.1%)	178 (59.7%)	1
	Low (IS-0/1)	3 (42.9%)	120 (40.3%)	
TLS activity	Active (maximum diameter of LAs ≥ 1 mm)	2 (28.6%)	68 (22.8%)	0.662
	Inactive (maximum diameter of LAs < 1 mm)	5 (71.4%)	230 (77.2%)	

Abbreviations: MSS, microsatellite stable; CRCs, colorectal carcinomas; AJCC/UICC, American Joint Committee on Cancer/Union for International Cancer Control; CIMP, CpG island methylator phenotype; CIMP−H, CIMP−high; CIMP−L/0, CIMP−low or negative; TIL, tumor−infiltrating lymphocyte; IS, immunoscore; TLS, tertiary lymphoid structure; LAs, lymphoid aggregates.

[a]Early recurrence was defined as tumor recurrence within two years after

curative surgery.

[b]One case was excluded from the *KRAS* mutation analysis results due to insufficient quantity of isolated DNA sample.

Table 2. Differential clinicopathologic, molecular, and immunologic characteristics of MSI-H CRCs according to CDX2 IHC expression status (n = 131)

Variable		CDX2 loss (n = 18)	CDX2 positive (n = 113)	*p*-value
Clinicopathologic factors				
Age	Older (≥ 64 years)	15 (83.3%)	61 (54.0%)	0.019
	Younger (< 64 years)	3 (16.7%)	52 (46.0%)	
Sex	Male	7 (38.9%)	57 (50.4%)	0.362
	Female	11 (61.1%)	56 (49.6%)	
Tumor location	Right-sided colon	15 (83.3%)	86 (76.1%)	0.763
	Left-sided colorectum	3 (16.7%)	27 (23.9%)	
Gross tumor type	Polypoid or fungating	8 (44.4%)	68 (60.2%)	0.209
	Ulceroinfiltrative	10 (55.6%)	45 (39.8%)	
Tumor size	Larger (≥ 6.4 cm)	6 (33.3%)	68 (60.2%)	0.033
	Smaller (< 6.4 cm)	12 (66.7%)	45 (39.8%)	
AJCC/UICC cancer stage	Stage I/II	10 (55.6%)	82 (72.6%)	0.143
	Stage III/IV	8 (44.4%)	31 (27.4%)	
Depth of invasion (pT)	Submucosa or proper muscle (pT1/pT2)	0 (0.0%)	17 (15.0%)	0.078
	Beyond the proper muscle (pT3/pT4)	18 (100.0%)	96 (85.0%)	
Lymph node metastasis (pN)	Absent (pN0)	10 (55.6%)	85 (75.2%)	0.094
	Present (pN1/pN2)	8 (44.4%)	28 (24.8%)	
Distant metastasis (pM or cM)	Absent (M0)	17 (94.4%)	104 (92.0%)	1.000
	Present (M1)	1 (5.6%)	9 (8.0%)	
Early recurrence	Absent	17 (94.4%)	104 (92.0%)	1.000

	Present	1 (5.6%)	9 (8.0%)	
Lymphatic invasion	Absent	7 (38.9%)	84 (74.3%)	0.002
	Present	11 (61.1%)	29 (25.7%)	
Venous invasion	Absent	16 (87.0%)	98 (86.7%)	0.796
	Present	2 (13.0%)	15 (13.3%)	
Perineural invasion	Absent	12 (66.7%)	85 (75.2%)	0.563
	Present	6 (33.3%)	28 (24.8%)	
Tumor differentiation	Well to moderately differentiated	6 (33.3%)	79 (69.9%)	0.003
	Poorly differentiated	12 (66.7%)	34 (30.1%)	
Mucinous histology	Non-mucinous (< 50%)	16 (88.9%)	80 (70.8%)	0.152
	Mucinous (≥ 50%)	2 (11.1%)	33 (29.2%)	
Signet ring cell histology	Absent	17 (94.4%)	95 (84.1%)	0.469
	Present	1 (5.6%)	18 (15.9%)	
Tumor budding	Low or intermediate	9 (50%)	86 (76.1%)	0.043
	High	9 (50%)	27 (23.9%)	
Poorly differentiated clusters	G1 or G2	5 (27.8%)	67 (59.3%)	0.020
	G3	13 (72.2%)	46 (40.7%)	
Desmoplastic reaction	Mature or intermediate	16 (88.9%)	108 (95.6%)	0.246
	Immature	2 (11.1%)	5 (4.4%)	
Molecular factors				
CIMP	CIMP-H	14 (77.8%)	31 (27.4%)	< 0.001
	CIMP-L/0	4 (22.2%)	82 (72.6%)	
MLH1 promoter methylation	Methylated	15 (83.3%)	43 (38.1%)	0.001
	Unmethylated	3 (16.7%)	70 (61.9%)	
CACNA1G promoter methylation	Methylated	13 (72.2%)	33 (29.2%)	0.001
	Unmethylated	5 (27.8%)	80 (70.8%)	
SOCS1 promoter methylation	Methylated	6 (33.3%)	37 (32.7%)	0.961

	Unmethylated	12 (66.7%)	76 (67.3%)	
CRABP1 promoter methylation	Methylated	16 (88.9%)	60 (53.1%)	0.004
	Unmethylated	2 (11.1%)	53 (46.9%)	
RUNX3 promoter methylation	Methylated	8 (44.4%)	30 (26.5%)	0.120
	Unmethylated	10 (55.6%)	83 (73.5%)	
IGF2 promoter methylation	Methylated	13 (72.2%)	27 (23.9%)	< 0.001
	Unmethylated	5 (27.8%)	86 (76.1%)	
CDKN2A promoter methylation	Methylated	13 (72.2%)	37 (32.7%)	0.001
	Unmethylated	5 (27.8%)	76 (67.3%)	
NEUROG1 promoter methylation	Methylated	15 (83.3%)	36 (31.9%)	< 0.001
	Unmethylated	3 (16.7%)	77 (68.1%)	
KRAS mutation	Absent	16 (88.9%)	70 (61.9%)	0.025
	Present	2 (11.1%)	43 (38.1%)	
BRAF mutation[a]	Absent	15 (83.3%)	101 (91%)	0.391
	Present	3 (16.7%)	10 (9%)	
SATB2 expression	Loss	7 (38.9%)	17 (15%)	0.023
	Positive	11 (61.1%)	96 (85%)	
KRT20 expression	Loss	12 (66.7%)	26 (23%)	< 0.001
	Positive	6 (33.3%)	87 (77%)	
Immunologic factors				
TIL immunoscore[b]	Intermediate to high (IS-2/3/4)	11 (61.1%)	61 (56.5%)	0.713
	Low (IS-0/1)	7 (38.9%)	47 (43.5%)	
TLS activity	Active (maximum diameter of LAs ≥ 1 mm)	10 (55.6%)	60 (53.1%)	0.846
	Inactive (maximum diameter of LAs < 1 mm)	8 (44.4%)	53 (46.9%)	

[a]Two cases were excluded from the BRAF mutation analysis results due to suboptimal quality or quantity of isolated DNA samples.

[b]Five cases were excluded from the TIL immunoscore results due to

suboptimal quality of immunohistochemistry slides.

Table 3. Differential clinicopathologic, molecular, and immunologic characteristics of MSS CRCs according to SATB2 IHC expression status (n = 305)

Variable		SATB2 loss (n = 14)	SATB2 positive (n = 291)	*p*-value
Clinicopathologic factors				
Age	Older (≥ 65 years)	8 (57.1%)	156 (53.6%)	0.796
	Younger (< 65 years)	6 (42.9%)	135 (46.4%)	
Sex	Male	7 (50.0%)	170 (58.4%)	0.533
	Female	7 (50.0%)	121 (41.6%)	
Tumor location	Right-sided colon	8 (57.1%)	58 (19.9%)	0.003
	Left-sided colorectum	6 (42.9%)	233 (80.1%)	
Gross tumor type	Polypoid or fungating	5 (35.7%)	121 (41.6%)	0.663
	Ulceroinfiltrative	9 (64.3%)	170 (58.4%)	
Tumor size	Larger (≥ 5.0 cm)	5 (35.7%)	148 (50.9%)	0.268
	Smaller (< 5.0 cm)	9 (64.3%)	143 (49.1%)	
AJCC/UICC cancer stage	Stage I/II	2 (14.3%)	132 (45.4%)	0.022
	Stage III/IV	12 (85.7%)	159 (54.6%)	
Depth of invasion (pT)	Submucosa or proper muscle (pT1/pT2)	0 (0.0%)	46 (15.8%)	0.106
	Beyond the proper muscle (pT3/pT4)	14 (100.0%)	245 (84.2%)	
Lymph node metastasis (pN)	Absent (pN0)	2 (14.3%)	140 (48.1%)	0.013
	Present (pN1/pN2)	12 (85.7%)	151 (51.9%)	
Distant metastasis (pM or cM)	Absent (M0)	7 (50.0%)	238 (81.8%)	0.009
	Present (M1)	7 (50.0%)	53 (18.2%)	
Early recurrence	Absent	11 (78.6%)	262 (90.3%)	0.161
	Present	3 (21.4%)	28 (9.7%)	

Lymphatic invasion	Absent	3 (21.4%)	189 (64.9%)	0.001
	Present	11 (78.6%)	102 (35.1%)	
Venous invasion	Absent	10 (71.4%)	226 (77.7%)	0.528
	Present	4 (28.6%)	65 (22.3%)	
Perineural invasion	Absent	3 (21.4%)	132 (45.4%)	0.078
	Present	11 (78.6%)	159 (54.6%)	
Tumor differentiation	Well to moderately differentiated	11 (78.6%)	273 (93.8%)	0.028
	Poorly differentiated	3 (21.4%)	18 (6.2%)	
Mucinous histology	Non-mucinous (< 50%)	14 (100.0%)	280 (96.6%)	1.000
	Mucinous (≥ 50%)	0 (0.0%)	10 (3.4%)	
Signet ring cell histology	Absent	14 (100.0%)	284 (97.9%)	1.000
	Present (≥ 5%)	0 (0.0%)	6 (2.1%)	
Tumor budding	Low or intermediate	1 (7.1%)	189 (65.2%)	< 0.001
	High	13 (92.9%)	101 (34.8%)	
Poorly differentiated clusters	G1 or G2	1 (7.1%)	137 (47.2%)	0.003
	G3	13 (92.9%)	153 (52.8%)	
Desmoplastic reaction	Mature or intermediate	11 (78.6%)	259 (89.3%)	0.197
	Immature	3 (21.4%)	31 (10.7%)	
Molecular factors				
CIMP	CIMP-H	4 (28.6%)	14 (4.8%)	0.006
	CIMP-L/0	10 (71.4%)	277 (95.2%)	
MLH1 promoter methylation	Methylated	0 (0.0%)	3 (1.0%)	1.000
	Unmethylated	14 (100.0%)	288 (99.0%)	
CACNA1G promoter methylation	Methylated	5 (35.7%)	18 (6.2%)	0.002
	Unmethylated	9 (64.3%)	273 (93.8%)	
SOCS1 promoter methylation	Methylated	1 (7.1%)	7 (2.4%)	0.316
	Unmethylated	13 (92.9%)	284 (97.6%)	

CRABP1 promoter methylation	Methylated	8 (57.1%)	64 (22.0%)	0.006
	Unmethylated	6 (42.9%)	227 (78.0%)	
RUNX3 promoter methylation	Methylated	2 (14.3%)	19 (6.5%)	0.249
	Unmethylated	12 (85.7%)	272 (93.5%)	
IGF2 promoter methylation	Methylated	6 (42.9%)	19 (6.5%)	<0.001
	Unmethylated	8 (57.1%)	272 (93.5%)	
CDKN2A promoter methylation	Methylated	6 (42.9%)	47 (16.2%)	0.020
	Unmethylated	8 (57.1%)	244 (83.8%)	
NEUROG1 promoter methylation	Methylated	6 (42.9%)	65 (22.3%)	0.101
	Unmethylated	8 (57.1%)	226 (77.7%)	
KRAS mutation[a]	Absent	3 (21.4%)	175 (60.3%)	0.004
	Present	11 (78.6%)	115 (39.7%)	
BRAF mutation	Absent	14 (100%)	286 (98.3%)	1
	Present	0 (0%)	5 (1.7%)	
CDX2 expression	Loss	1 (7.1%)	6 (2.1%)	0.283
	Positive	13 (92.9%)	285 (97.9%)	
KRT20 expression	Loss	2 (14.3%)	19 (6.5%)	0.249
	Positive	12 (85.7%)	272 (93.5%)	
Immunologic factors				
TIL immunoscore	Intermediate to high (IS-2/3/4)	4 (28.6%)	178 (61.2%)	0.015
	Low (IS-0/1)	10 (71.4%)	113 (38.8%)	
TLS activity	Active (maximum diameter of LAs ≥ 1 mm)	1 (7.1%)	69 (23.7%)	0.203
	Inactive (maximum diameter of LAs < 1 mm)	13 (92.9%)	222 (76.3%)	

[a]One case was excluded from the *KRAS* mutation analysis results due to insufficient quantity of isolated DNA sample.

Table 4. Differential clinicopathologic, molecular, and immunologic characteristics of MSI-H CRCs according to SATB2 IHC expression status (n = 131)

Variable		SATB2 loss (n = 24)	SATB2 positive (n = 107)	*p*-value
Clinicopathologic factors				
Age	Older (≥ 64 years)	16 (66.7%)	60 (56.1%)	0.342
	Younger (< 64 years)	8 (33.3%)	47 (43.9%)	
Sex	Male	12 (50.0%)	52 (48.6%)	0.901
	Female	12 (50.0%)	55 (51.4%)	
Tumor location	Right-sided colon	19 (79.2%)	82 (76.6%)	0.79
	Left-sided colorectum	5 (20.8%)	25 (23.4%)	
Gross tumor type	Polypoid or fungating	13 (54.2%)	63 (58.9%)	0.673
	Ulceroinfiltrative	11 (45.8%)	44 (41.1%)	
Tumor size	Larger (≥ 6.4 cm)	13 (54.2%)	44 (41.1%)	0.244
	Smaller (< 6.4 cm)	11 (45.8%)	63 (58.9%)	
AJCC/UICC cancer stage	Stage I/II	15 (62.5%)	77 (72.0%)	0.360
	Stage III/IV	9 (37.5%)	30 (28.0%)	
Depth of invasion (pT)	Submucosa or proper muscle (pT1/pT2)	0 (0.0%)	17 (15.9%)	0.041
	Beyond the proper muscle (pT3/pT4)	24 (100.0%)	90 (84.1%)	
Lymph node metastasis (pN)	Absent (pN0)	16 (66.7%)	79 (73.8%)	0.477
	Present (pN1/pN2)	8 (33.3%)	28 (26.2%)	
Distant metastasis (pM or cM)	Absent (M0)	22 (91.7%)	99 (92.5%)	1.000
	Present (M1)	2 (18.3%)	8 (7.5%)	
Early recurrence	Absent	20 (83.3%)	101 (94.4%)	0.085
	Present	4 (16.7%)	6 (5.6%)	
Lymphatic invasion	Absent	11 (45.8%)	80 (74.8%)	0.005
	Present	13 (54.2%)	27 (25.2%)	

Venous invasion	Absent	21 (87.5%)	93 (86.9%)	1.000
	Present	3 (12.5%)	14 (13.1%)	
Perineural invasion	Absent	16 (66.7%)	81 (75.7%)	0.362
	Present	8 (33.3%)	26 (24.3%)	
Tumor differentiation	Well to moderately differentiated	12 (50%)	73 (68.2%)	0.091
	Poorly differentiated	12 (50%)	34 (31.8%)	
Mucinous histology	Non-mucinous (< 50%)	17 (70.8%)	79 (73.8%)	0.764
	Mucinous (≥ 50%)	7 (29.2%)	28 (26.2%)	
Signet ring cell histology	Absent	16 (66.7%)	96 (89.7%)	0.004
	Present	8 (33.3%)	11 (10.3%)	
Tumor budding	Low or intermediate	15 (62.5%)	80 (74.8%)	0.224
	High	9 (37.5%)	27 (25.2%)	
Poorly differentiated clusters	G1 or G2	11 (45.8%)	61 (57.0%)	0.320
	G3	13 (54.2%)	46 (43.0%)	
Desmoplastic reaction	Mature or intermediate	21 (87.5%)	103 (96.3%)	0.115
	Immature	3 (12.5%)	4 (3.7%)	
Molecular factors				
CIMP	CIMP-H	13 (54.2%)	32 (29.9%)	0.024
	CIMP-L/0	11 (45.8%)	75 (70.1%)	
MLH1 promoter methylation	Methylated	12 (50.0%)	46 (43.0%)	0.532
	Unmethylated	12 (50.0%)	61 (57.0%)	
CACNA1G promoter methylation	Methylated	13 (54.2%)	33 (30.8%)	0.030
	Unmethylated	11 (45.8%)	74 (69.2%)	
SOCS1 promoter methylation	Methylated	7 (29.2%)	36 (33.6%)	0.673
	Unmethylated	17 (70.8%)	71 (66.4%)	
CRABP1 promoter methylation	Methylated	17 (70.8%)	59 (55.1%)	0.159
	Unmethylated	7 (29.2%)	48 (44.9%)	

RUNX3 promoter methylation	Methylated	11 (45.8%)	27 (25.2%)	0.044
	Unmethylated	13 (54.2%)	80 (74.8%)	
IGF2 promoter methylation	Methylated	12 (50.0%)	28 (26.2%)	0.022
	Unmethylated	12 (50.0%)	79 (73.8%)	
CDKN2A promoter methylation	Methylated	11 (45.8%)	39 (36.4%)	0.392
	Unmethylated	13 (54.2%)	68 (63.6%)	
NEUROG1 promoter methylation	Methylated	15 (62.5%)	36 (33.6%)	0.009
	Unmethylated	9 (37.5%)	71 (66.4%)	
KRAS mutation	Absent	19 (79.2%)	67 (62.6%)	0.123
	Present	5 (20.8%)	40 (37.4%)	
BRAF mutation[a]	Absent	19 (82.6%)	97 (91.5%)	0.247
	Present	4 (17.4%)	9 (8.5%)	
CDX2 expression	Loss	8 (33.3%)	11 (10.3%)	0.008
	Positive	16 (66.7%)	96 (89.7%)	
KRT20 expression	Loss	10 (41.7%)	28 (26.2%)	0.131
	Positive	14 (58.3%)	79 (73.8%)	
Immunologic factors				
TIL immunoscore[b]	Intermediate to high (IS-2/3/4)	13 (56.5%)	59 (57.3%)	0.947
	Low (IS-0/1)	10 (43.5%)	44 (42.7%)	
TLS activity	Active (maximum diameter of LAs ≥ 1 mm)	14 (58.3%)	56 (52.3%)	0.595
	Inactive (maximum diameter of LAs < 1 mm)	10 (41.7%)	51 (47.7%)	

[a]Two cases were excluded from the *BRAF* mutation analysis results due to suboptimal quality or quantity of isolated DNA samples.

[b]Five cases were excluded from the TIL immunoscore results due to suboptimal quality of immunohistochemistry slides.

Table 5. Differential clinicopathologic, molecular, and immunologic characteristics of MSS CRCs according to KRT20 IHC expression status (n = 305)

Variable		KRT20 loss (n = 21)	KRT20 positive (n = 284)	*p*-value
Clinicopathologic factors				
Age	Older (≥ 65 years)	11 (52.4%)	153 (53.9%)	0.895
	Younger (< 65 years)	10 (47.6%)	131 (46.1%)	
Sex	Male	10 (47.6%)	167 (58.8%)	0.316
	Female	11 (52.4%)	117 (41.2%)	
Tumor location	Right-sided colon	9 (42.9%)	57 (20.1%)	0.025
	Left-sided colorectum	12 (57.1%)	227 (79.9%)	
Gross tumor type	Polypoid or fungating	9 (42.9%)	117 (41.2%)	0.881
	Ulceroinfiltrative	12 (57.1%)	167 (58.8%)	
Tumor size	Larger (≥ 5.0 cm)	17 (81.0%)	136 (47.9%)	0.003
	Smaller (< 5.0 cm)	4 (19.0%)	148 (52.1%)	
AJCC/UICC cancer stage	Stage I/II	10 (47.6%)	124 (43.7%)	0.724
	Stage III/IV	11 (52.4%)	160 (56.3%)	
Depth of invasion (pT)	Submucosa or proper muscle (pT1/pT2)	2 (9.5%)	44 (15.5%)	0.751
	Beyond the proper muscle (pT3/pT4)	19 (90.5%)	240 (84.5%)	
Lymph node metastasis (pN)	Absent (pN0)	10 (47.6%)	132 (46.5%)	0.919
	Present (pN1/pN2)	11 (52.4%)	152 (53.5%)	
Distant metastasis (pM or cM)	Absent (M0)	17 (81.0%)	228 (80.3%)	1.000
	Present (M1)	4 (19.0%)	56 (19.7%)	
Early recurrence	Absent	17 (85.0%)	256 (90.1%)	0.442
	Present	3 (15.0%)	28 (9.9%)	
Lymphatic invasion	Absent	12 (57.1%)	180 (63.4%)	0.568
	Present	9 (42.9%)	104 (36.6%)	

Venous invasion	Absent	16 (76.2%)	220 (77.5%)	1.000
	Present	5 (23.8%)	64 (22.5%)	
Perineural invasion	Absent	14 (66.7%)	121 (42.6%)	0.032
	Present	7 (33.3%)	163 (57.4%)	
Tumor differentiation	Well to moderately differentiated	16 (76.2%)	268 (94.4%)	0.009
	Poorly differentiated	5 (23.8%)	16 (5.6%)	
Mucinous histology	Non-mucinous (< 50%)	20 (95.2%)	275 (96.8%)	0.515
	Mucinous (≥ 50%)	1 (4.8%)	9 (3.2%)	
Signet ring cell histology	Absent	21 (100.0%)	277 (97.9%)	1.000
	Present	0 (0.0%)	6 (2.1%)	
Tumor budding	Low or intermediate	12 (57.1%)	178 (62.9%)	0.599
	High	9 (42.9%)	105 (37.1%)	
Poorly differentiated clusters	G1 or G2	8 (38.1%)	130 (45.9%)	0.486
	G3	13 (61.9%)	153 (54.1%)	
Desmoplastic reaction	Mature or intermediate	20 (95.2%)	250 (88.3%)	0.488
	Immature	1 (4.8%)	33 (11.7%)	
Molecular factors				
CIMP	CIMP-H	3 (14.3%)	15 (5.3%)	0.091
	CIMP-L/0	18 (85.7%)	269 (94.7%)	
MLH1 promoter methylation	Methylated	1 (4.8%)	2 (0.7%)	0.193
	Unmethylated	20 (95.2%)	282 (99.3%)	
CACNA1G promoter methylation	Methylated	3 (14.3%)	20 (7.0%)	0.203
	Unmethylated	18 (85.7%)	264 (93.0%)	
SOCS1 promoter methylation	Methylated	0 (0.0%)	8 (2.8%)	1.000
	Unmethylated	21 (100.0%)	276 (97.2%)	
CRABP1 promoter methylation	Methylated	11 (52.4%)	61 (21.5%)	0.003
	Unmethylated	10 (47.6%)	223 (78.5%)	

RUNX3 promoter methylation	Methylated	6 (28.6%)	15 (5.3%)	0.001
	Unmethylated	15 (71.4%)	269 (94.7%)	
IGF2 promoter methylation	Methylated	5 (23.8%)	20 (7.0%)	0.020
	Unmethylated	16 (76.2%)	264 (93.0%)	
CDKN2A promoter methylation	Methylated	7 (33.3%)	46 (16.2%)	0.067
	Unmethylated	14 (66.7%)	238 (83.8%)	
NEUROG1 promoter methylation	Methylated	5 (23.8%)	66 (23.2%)	1.000
	Unmethylated	16 (76.2%)	218 (76.8%)	
KRAS mutation[a]	Absent	10 (47.6%)	168 (59.4%)	0.292
	Present	11 (52.4%)	115 (40.6%)	
BRAF mutation	Absent	20 (95.2%)	280 (98.6%)	0.302
	Present	1 (4.8%)	4 (1.4%)	
CDX2 expression	Loss	1 (4.8%)	6 (2.1%)	0.396
	Positive	20 (95.2%)	278 (97.9%)	
SATB2 expression	Loss	2 (9.5%)	12 (4.2%)	0.249
	Positive	19 (90.5%)	272 (95.8%)	
Immunologic factors				
TIL immunoscore	Intermediate to high (IS-2/3/4)	14 (66.7%)	168 (59.2%)	0.498
	Low (IS-0/1)	7 (33.3%)	116 (40.8%)	
TLS activity	Active (maximum diameter of LAs ≥ 1 mm)	8 (38.1%)	62 (21.8%)	0.197
	Inactive (maximum diameter of LAs < 1 mm)	13 (61.9%)	222 (78.2%)	

[a]One case was excluded from the *KRAS* mutation analysis results due to insufficient quantity of isolated DNA samples.

Table 6. Differential clinicopathologic, molecular, and immunologic characteristics of MSI-H CRCs according to KRT20 IHC expression status (n = 131)

Variable		KRT20 loss (n = 38)	KRT20 positive (n = 93)	*p*-value
Clinicopathologic factors				
Age	Older (≥ 64 years)	26 (68.4%)	50 (53.8%)	0.123
	Younger (< 64 years)	12 (31.6%)	43 (46.2%)	
Sex	Male	16 (42.1%)	48 (51.6%)	0.323
	Female	22 (57.9%)	45 (48.4%)	
Tumor location	Right-sided colon	30 (78.9%)	71 (76.3%)	0.748
	Left-sided colorectum	8 (21.1%)	22 (23.7%)	
Gross tumor type	Polypoid or fungating	17 (44.7%)	59 (63.4%)	0.049
	Ulceroinfiltrative	21 (55.3%)	34 (36.6%)	
Tumor size	Larger (≥ 6.4 cm)	18 (47.4%)	39 (41.9%)	0.569
	Smaller (< 6.4 cm)	20 (52.6%)	54 (58.1%)	
AJCC/UICC cancer stage	Stage I/II	22 (57.9%)	70 (75.3%)	0.048
	Stage III/IV	16 (42.1%)	23 (24.7%)	
Depth of invasion (pT)	Submucosa or proper muscle (pT1/pT2)	1 (2.6%)	16 (17.2%)	0.023
	Beyond the proper muscle (pT3/pT4)	37 (97.4%)	77 (82.8%)	
Lymph node metastasis (pN)	Absent (pN0)	24 (63.2%)	71 (76.3%)	0.125
	Present (pN1/pN2)	14 (36.8%)	22 (23.7%)	
Distant metastasis (pM or cM)	Absent (M0)	34 (89.5%)	87 (93.5%)	0.475
	Present (M1)	4 (10.5%)	6 (6.5%)	
Early recurrence	Absent	33 (86.8%)	87 (93.5%)	0.296
	Present	5 (13.2%)	6 (6.5%)	
Lymphatic invasion	Absent	20 (52.6%)	71 (76.3%)	0.007

	Present	18 (47.4%)	22 (23.7%)	
Venous invasion	Absent	36 (94.7%)	78 (83.9%)	0.15
	Present	2 (5.3%)	15 (16.1%)	
Perineural invasion	Absent	25 (65.8%)	72 (77.4%)	0.168
	Present	13 (34.2%)	21 (22.6%)	
Tumor differentiation	Well to moderately differentiated	19 (50%)	66 (71%)	0.023
	Poorly differentiated	19 (50%)	27 (29%)	
Mucinous histology	Non-mucinous (< 50%)	33 (86.8%)	63 (67.7%)	0.025
	Mucinous (≥ 50%)	5 (13.2%)	30 (32.3%)	
Signet ring cell histology	Absent	33 (86.8%)	79 (84.9%)	0.78
	Present	5 (13.2%)	14 (15.1%)	
Tumor budding	Low or intermediate	24 (63.2%)	71 (76.3%)	0.125
	High	14 (36.8%)	22 (23.7%)	
Poorly differentiated clusters	G1 or G2	18 (47.4%)	56 (60.2%)	0.178
	G3	20 (52.6%)	37 (39.8%)	
Desmoplastic reaction	Mature or intermediate	34 (89.5%)	90 (96.8%)	0.192
	Immature	4 (10.5%)	3 (3.2%)	
Molecular factors				
CIMP	CIMP-H	21 (55.3%)	24 (25.8%)	0.001
	CIMP-L/0	17 (44.7%)	69 (74.2%)	
MLH1 promoter methylation	Methylated	23 (60.5%)	35 (37.6%)	0.017
	Unmethylated	15 (39.5%)	58 (62.4%)	
CACNA1G promoter methylation	Methylated	20 (52.6%)	26 (28.0%)	0.007
	Unmethylated	18 (47.4%)	67 (72.0%)	
SOCS1 promoter methylation	Methylated	14 (36.8%)	29 (31.2%)	0.531
	Unmethylated	24 (63.2%)	64 (68.8%)	
CRABP1 promoter methylation	Methylated	28 (73.7%)	48 (51.6%)	0.02

	Unmethylated	10 (26.3%)	45 (48.4%)	
RUNX3 promoter methylation	Methylated	17 (44.7%)	21 (22.6%)	0.011
	Unmethylated	21 (55.3%)	72 (77.4%)	
IGF2 promoter methylation	Methylated	17 (44.7%)	23 (24.7%)	0.024
	Unmethylated	21 (55.3%)	70 (75.3%)	
CDKN2A promoter methylation	Methylated	23 (60.5%)	27 (29.0%)	0.001
	Unmethylated	15 (39.5%)	66 (71.0%)	
NEUROG1 promoter methylation	Methylated	21 (55.3%)	30 (32.3%)	0.014
	Unmethylated	17 (44.7%)	63 (67.7%)	
KRAS mutation	Absent	31 (81.6%)	55 (59.1%)	0.014
	Present	7 (18.4%)	38 (40.9%)	
BRAF mutation[a]	Absent	31 (86.1%)	85 (91.4%)	0.351
	Present	5 (13.9%)	8 (8.6%)	
CDX2 expression	Loss	13 (34.2%)	6 (6.5%)	< 0.001
	Positive	25 (65.8%)	87 (93.5%)	
SATB2 expression	Loss	10 (26.3%)	14 (15.1%)	0.131
	Positive	28 (73.7%)	79 (84.9%)	
Immunologic factors				
TIL immunoscore[b]	Intermediate to high (IS-2/3/4)	20 (55.6%)	52 (57.8%)	0.82
	Low (IS-0/1)	16 (44.4%)	38 (42.2%)	
TLS activity	Active (maximum diameter of LAs ≥ 1 mm)	21 (55.3%)	49 (52.7%)	0.789
	Inactive (maximum diameter of LAs < 1 mm)	17 (44.7%)	44 (47.3%)	

[a]Two cases were excluded from the BRAF mutation analysis results due to suboptimal quality or quantity of isolated DNA samples.

[b]Five cases were excluded from the TIL immunoscore results due to suboptimal quality of immunohistochemistry slides.

Characterization of CDX2−/SATB2−/KRT20−(triple−negative) CRCs

The simultaneous loss of CDX2, SATB2, and KRT20 expression (CDX2−/SATB2−/KRT20−; the triple−negative phenotype) was observed in 6 out of 131 MSI−H CRCs (4.6%; Fig. 4a and Fig. 5a). All triple−negative tumors were confirmed to be primary CRCs without evidence of other extra−colorectal tumors. The major clinicopathologic and molecular features of the six triple−negative tumors are summarized in Table 7. Various histologic subtypes, including signet ring cell, medullary, and serrated types, were observed in the triple−negative CRCs (Table 7 and Fig. 6). Notably, all six triple−negative CRCs commonly displayed molecular profiles of sporadic MSI−H subtype such as CIMP−H and MLH1 promoter methylation, with loss of MLH1 IHC expression (Table 7 and Fig. 5a). Consistent with the known clinical characteristics of sporadic MSI−H CRCs, all the triple−negative CRC patients were old (average age, 76 years; range, 67-89 years) and except for one patient, all were females (Table 7). The triple−negative tumors were exclusively located in the proximal colon and frequently showed poor differentiation (Table 7). In two cases, KRT7 IHC expression was observed in the tumor cells (Fig. 5a).

Finally, we confirmed that the IHC profiles of primary triple−negative CRCs, including CDX2/SATB2/KRT20/MLH1 loss, were maintained in the corresponding metastatic lymph node (Fig. 5b).

Figure 5. Pathology of CRCs showing concurrent loss of all the three intestinal markers (triple−negative)

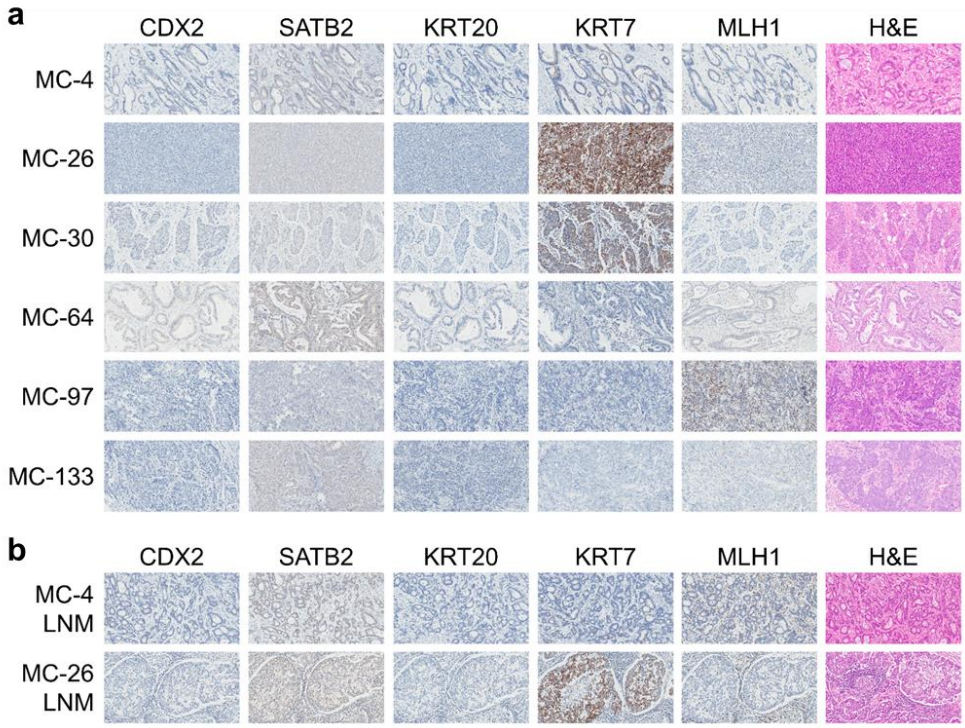

a IHC and H&E photomicrographs of primary tumor issues of the triple−negative CRCs. Note the common loss of MLH1 IHC expression in the tumor cells of all six cases. b IHC and H&E photomicrographs of lymph node metastatic tumor tissues of the stage III triple−negative CRCs. Note the consistency of IHC profiles between matched primary and metastatic tumor tissues of the two cases (MC−4 and MC−26)

Figure 6. Detailed histopathologic features of triple-negative colorectal carcinomas

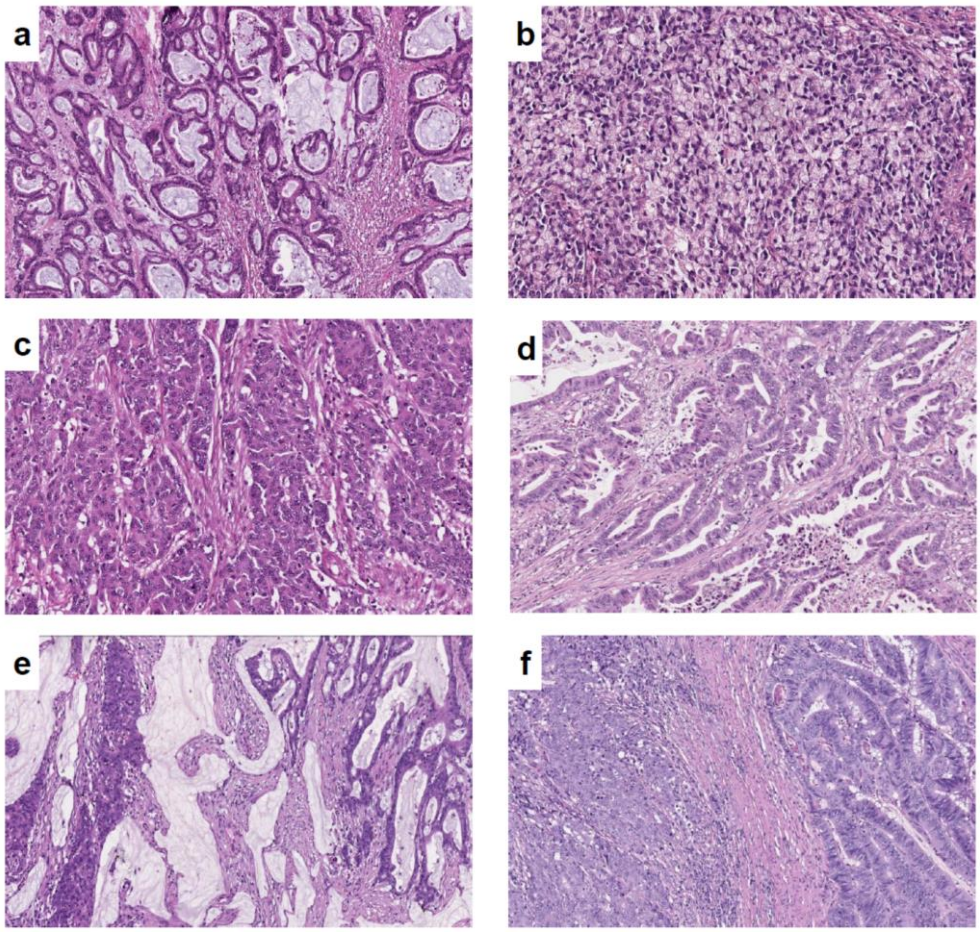

a An adenocarcinoma with focal intraglandular mucin production (MC-4). **b** A signet ring cell carcinoma with prominent intracytoplasmic mucin (MC-26). **c** A medullary carcinoma with solid growth and tumor-infiltrating lymphocytes (MC-30). **d** A serrated adenocarcinoma showing luminal serrated morphology in glands (MC-64). **e** An adenocarcinoma with focal extracellular mucin production (MC-97). **f** An adenocarcinoma with focal medullary feature (MC-133).

Table 7. Clinicopathologic and molecular characteristics of triple-negative (CDX2-/SATB2-/KRT20-) CRCs

Case No.	Age	Sex	Tumor location	Histologic type	Histologic differentiation	Mucin production	TNM stage (AJCC 8th)	MSI	CIMP	*MLH1* methylation / MLH1 IHC	*BRAF* mutation	*KRAS* mutation
MC-4	76	Female	Ascending colon	Adenocarcinoma	Moderately differentiated	Present, focal (<50%)	pT4aN1a cM0	MSI-H	CIMP-H	Methylated / Loss	Wild-type	Wild-type
MC-26	89	Female	Hepatic flexure	Signet ring cell carcinoma	Poorly differentiated	Present, focal (<50%)	pT3cN1a cM0	MSI-H	CIMP-H	Methylated / Loss	Wild-type	Wild-type
MC-30	67	Female	Ascending colon	Adenocarcinoma	Poorly differentiated	Absent	pT3bN0 cM0	MSI-H	CIMP-H	Methylated / Loss	Wild-type	Wild-type
MC-64	83	Female	Ascending colon	Serrated adenocarcinoma	Moderately differentiated	Absent	pT3bN0 cM0	MSI-H	CIMP-H	Methylated / Loss	Mutant (p.V600E)	Wild-type
MC-97	72	Male	Ascending colon	Adenocarcinoma	Poorly differentiated	Present, focal (<50%)	pT3aN0 cM0	MSI-H	CIMP-H	Methylated / Loss	Mutant (p.V600E)	Wild-type
MC-133	71	Female	Ascending colon	Adenocarcinoma	Poorly differentiated	Present, focal (<50%)	pT3cN0 cM0	MSI-H	CIMP-H	Methylated / Loss	Wild-type	Wild-type

Chapter3. Conclusion

In this study, we comprehensively characterized the clinicopathologic and molecular factors associated with alterations in the expression of three intestinal epithelium-specific markers (CDX2, SATB2, and KRT20) at both RNA and protein levels in CRCs. Analysis of TCGA CRC data (n=390) revealed that decreased mRNA expression of the three intestinal marker genes commonly correlated with MSI-H, CIMP-H, BRAF/RNF43 mutations, CMS1, and high TMB (Fig. 2), which collectively reflect features of sporadic MSI-H CRCs because CMS1 and high TMB are representative MSI-H-dependent factors in CRC. Moreover, CIMP-H and BRAF/RNF43 mutations are prevalent specifically in MLH1-methylated sporadic MSI-H CRCs, but not in hereditary MSI-H CRCs of Lynch syndrome [42-46]. From these findings, we can confirm two principles regarding the loss of intestinal markers in CRC. (1) The decreased expression of intestinal markers in subsets of CRCs is initiated at the RNA transcriptional level. (2) The decreased expression of intestinal markers in CRCs is associated with a specific carcinogenesis pathway resulting in sporadic MSI-H CRCs, which is also known as the sessile serrated neoplasia pathway [47].

The loss of CDX2 and SATB2 IHC expression in CRC tissues was commonly associated with CIMP-H and lymphatic invasion regardless of MSI status (Fig. 4b), whereas loss of KRT20 expression was significantly correlated with poor differentiation regardless of MSI status (Fig. 4b). Similar features between CDX2 loss and SATB2 loss and different natures between CDX2/SATB2 loss and KRT20 loss in CRCs were also confirmed by the comparative analysis of MSI/CIMP subgroups of CRCs; both CDX2 and SATB2 expressions were decreased in CIMP-H subgroups regardless of MSI status, whereas KRT20 expression was decreased in MSI-H subgroups regardless of CIMP status (Fig. 3c). Previous multivariate analysis studies have also reported that the loss of CDX2 expression is associated with CIMP-H but not MSI-H in CRCs [12, 25].

However, CIMP-H-dependent/MSI-H-independent expression alterations of CDX2 and SATB2 observed in the IHC analysis were unclear in the RNA expression analysis (Fig. 1d). It is likely that the reduced expression of *CDX2/SATB2* mRNA may be affected by both MSI-H and CIMP-H status in CRCs because, except for the MSS/CIMP-L/0 subgroup, the other three subgroups with MSI-H and/or CIMP-H displayed decreased mRNA expression of *CDX2* and *SATB2* genes (Fig. 1d). To consider the mechanism of decreased mRNA expression, we analyzed promoter methylation of SATB2 and SATB2 mRNA expression in TCGA samples and confirmed inverse correlation between two. Also, Xu et al. showed that the enrichment of H3K4me3 in the SATB2 promoter region was significantly reduced in the CRC tissues [51].

The discrepancy between protein-level and RNA-level results may be due to potential direct or indirect interactions between transcription factors (TFs) and CIMP-H in CRCs. Both CDX2 and SATB2 are TFs associated with intestinal differentiation during normal development [48, 49], whereas KRT20 is a filament protein that supports the structural integrity of intestinal epithelial cells [11]. Thus, we postulate that the expression of CDX2 and SATB2, and not KRT20, may be further decreased by epigenetic or posttranslational modifications, particularly under CIMP-H conditions in CRC. CIMP-H is an epigenetic change associated with the suppression of gene expression by promoter CpG island hypermethylation in cancers [42], and DNA methylation is known to be associated with other epigenetic/post-translational alterations such as chromatin structure changes, histone modifications, or non-coding RNA regulation, which may also be associated with aberrations in the normal binding and expression of TFs [50].

Also, several studies have reported that SATB2 expression in CRC is regulated by long non-coding RNA (SATB2-AS1) or microRNAs (miR-31, miR-34, miR-182, miR-211, and miR-599) [49, 51-53]. CDX2 expression is also suggested to be regulated by epigenetic mechanisms such as promoter methylation or histone modifications [16, 54, 55]. Collectively, in contrast to KRT20, both CDX2 and

SATB2 are TFs, and their protein-level expression may be affected by epigenetic or post-translational modifications frequently in CIMP-H CRCs.

Interestingly, in addition to the differences between CDX2/SATB2 loss and KRT20 loss in CRCs, we also observed differences in several clinicopathologic and molecular aspects between CDX2 loss and SATB2 loss in CRCs. Although both CDX2 and SATB2 are intestinal differentiation-related TFs and their loss of expression is commonly associated with CIMP-H in CRCs (Fig. 4b), CDX2 loss was not significantly correlated with SATB2 loss in MSS CRCs ($p = 0.283$; Fig. 4b). In addition, the frequency of concurrent loss of CDX2 and SATB2 expression was relatively low in both MSI-H and MSS CRCs (5.4% and 0.3%, respectively) compared with the frequency of the loss of CDX2 or SATB2 alone (Fig. 4a). Similar to our findings, Ma et al. previously reported that the concurrent loss of CDX2 and SATB2 expression was observed in only 6% and 2% of MSI-H and MSS CRCs, respectively [23]. These features indicate that tumors with CDX2 loss and tumor with SATB2 loss comprise distinct subsets within CIMP-H CRCs. The clinicopathologic and molecular differences between CDX2-loss tumors and STAB2-loss tumors further confirmed that in MSS CRCs, CDX2 loss was significantly associated with *BRAF* V600E mutation whereas SATB2 loss with *KRAS* mutations and low TIL immunoscore (Fig. 4b, c). Although the underlying mechanism of the association between SATB2 loss and low TIL density in MSS CRCs is yet to be elucidated, the high incidence of KRAS mutations (78.6%; Table 3) in SATB2-loss MSS CRCs may be a potential underlying factor for impaired antitumor immunity as recent studies have suggested that *KRAS* mutations are associated with immune suppression in CRCs [56, 57].

In the differential diagnosis of metastatic carcinomas having multiple possibilities for the site of the primary tumor, including the colorectum, metastatic CRC showing the concurrent loss of all the three intestinal markers (triple-negative) can lead to great confusion and misdiagnosis. All six triple-negative CRCs evaluated in our study were found exclusively in the *MLH1*-methylated MSI-H/CIMP-H

molecular subtype of CRCs (sporadic MSI-H CRCs) (Table 7). Because CDX2/SATB2 loss and KRT20 loss in CRC were revealed to be dependent on CIMP-H and MSI-H status, respectively, it is reasonable that the triple-negative tumors were found in an overlap zone-in CRC with both MSI-H and CIMP-H. Age (67–89 years), sex (female, 83%), and tumor location (right-sided colon, 100%) may be clinical clues, and poor differentiation (67%) and loss of MLH1 IHC expression (100%) could be pathologic clues for the triple-negative tumors (Table 7 and Fig. 5). These clues can aid diagnosis and the identification of the primary site of metastatic carcinomas showing unusual expression profiles of tissue-specific markers, especially in rare and difficult to diagnose triple-negative CRCs.

Among the six triple-negative CRCs, two cases, which were non-medullary carcinomas, showed lymph node metastases (Table 7). Considering that MSI-H CRCs demonstrate relatively low frequencies of nodal/distant metastases and generally show a favorable prognosis, our finding suggests that triple-negative CRCs without medullary histology may represent an aggressive MSI-H subset. Due to short follow up period after the surgery, 5-year overall survival data is analyzed only in 76 MSI-H CRC cases. Double- or triple-negative cases tend to have poor outcome although statistically not significant. We also investigated whether patients with triple-negative CRCs had distant metastases or recurrence during their follow-up periods, and observed that none of the patients showed any evidence of distant metastases. However, the absence of metastatic or recurrent triple-negative CRCs rarely metastasize to distant sites is also important because if the triple intestinal markers are all negative in a carcinoma of undetermined primary, the likelihood of the colorectal origin of the tumor is extremely rare.

Our study identified comprehensive clinicopathologic and molecular characteristics of CRCs showing loss of intestinal marker expression; however, there are several limitations to it. First, to investigate the RNA-level and protein-level features of intestinal markers in CRC, we used different sample cohorts—TCGA cohort (n = 390) for RNA

data and primary tissue cohorts (n = 436) for protein data. The clinicopathologic and molecular correlates of RNA-level and protein-level expression alterations of intestinal markers in CRC might be well characterized in our study because relatively large numbers of CRCs were used in analyzing both TCGA CRC and primary CRC cohorts. However, a direct comparison between RNA-level and protein-level alterations of intestinal markers in CRC was not performed. Further investigation is warranted to confirm the similarities and dissimilarities between RNA-level and protein-level alterations of intestinal markers in CRC. The second limitation of our study is the potential bias due to TMA-based IHC evaluation. To evaluate the IHC expression of intestinal markers in the 436 CRCs, we used TMA slides instead of whole tumor slides. To minimize the disadvantage of a TMA core being less representative of the entire tumor area, we stained each intestinal marker IHC using four TMA cores from different tumor areas (two at the IM and two at the CT). Despite our efforts with using multi-core TMA slides, the possibility that the intratumoral heterogeneity of IHC expression was incompletely reflected cannot be entirely excluded. The precise evaluation of the expression patterns of intestinal markers in the whole tumor area of CRC warrants further validation studies using whole slide IHC.

In conclusion, out study revealed that the decreased mRNA expression of *CDX2* and *SATB2* is associated with both MSI-H and CIMP-H in CRC, whereas the loss of protein expression of CDX2 and SATB2 was more dependent on CIMP-H than MSI-H in CRC. In contrast, decreased expression of both *KRT20* mRNA and protein was associated more with MSI-H than CIMP-H in CRC. We also found that clinicopathologic and molecular characteristics associated with the loss of intestinal markers could be different in relation to MSI status. *KRAS* mutations and low TILs, which are important factors affecting responses to targeted therapy and immunotherapy, respectively, were associated with SATB2 loss in MSS CRCs, and further studies will be needed to explore therapeutic implications of SATB2 loss in CRCs. CRCs showing concurrent loss of

CDX2/SATB2/KRT20 IHC expression were found to occur exclusively in proximal colon-located MSI-H/CIMP-H cancers with *MLH1* promoter methylation. Our data provide important information regarding the factors to be considered in the differential diagnosis of metastatic CRCs with loss of intestinal marker expression.

Bibliography

1. Siegel RL, Miller KD, Fuchs HE, Jemal A (2021) Cancer statistics, 2021. CA Cancer J Clin 71:7–33. https://doi.org/10.3322/caac.21654
2. van der Geest LG, Lam−Boer J, Koopman M, Verhoef C, Elferink MA, de Wilt JH (2015) Nationwide trends in incidence, treatment and survival of colorectal cancer patients with synchronous metastases. Clin Exp Metastasis 32:457–465. https://doi.org/10.1007/ s10585−015−9719−0
3. van Gestel YR, de Hingh IH, van Herk−Sukel MP, van Erning FN, Beerepoot LV, Wijsman JH, Slooter GD, Rutten HJ, Creemers GJ, Lemmens VE (2014) Patterns of metachronous metastases after curative treatment of colorectal cancer. Cancer Epidemiol 38:448–454. https://doi.org/10.1016/j.canep.2014.04.004
4. Moskaluk CA, Zhang H, Powell SM, Cerilli LA, Hampton GM, Frierson HF Jr (2003) Cdx2 protein expression in normal and malignant human tissues: an immunohistochemical survey using tissue microarrays. Mod Pathol 16:913–919. https://doi.org/10.1097/01.MP.00000 86073.92773.55
5. Werling RW, Yaziji H, Bacchi CE, Gown AM (2003) CDX2, a highly sensitive and specific marker of adenocarcinomas of intestinal origin: an immunohistochemical survey of 476 primary and metastatic carcinomas. Am J Surg Pathol 27:303–310. https://doi.org/10.1097/00000478−200303000−00003
6. Kaimaktchiev V, Terracciano L, Tornillo L, Spichtin H, Stoios D, Bundi M, Korcheva V, Mirlacher M, Loda M, Sauter G, Corless CL (2004) The homeobox intestinal differentiation factor CDX2 is selectively expressed in gastrointestinal adenocarcinomas. Mod Pathol 17:1392–1399. https://doi.org/10.1038/modpathol.3800205
7. De Lott LB, Morrison C, Suster S, Cohn DE, Frankel WL (2005) CDX2 is a useful marker of intestinal−type differentiation−a tissue microarray−based study of 629 tumors from various sites. Arch Pathol Lab Med 129:1100–1105
8. Dennis JL, Hvidsten TR, Wit EC, Komorowski J, Bell AK, Downie I, Mooney J, Verbeke C, Bellamy C, Keith WN, Olien KA (2005)

Markers of adenocarcinoma characteristic of the site of origin: development of a diagnostic algorithm. Clin Cancer Res 11:3766–3772. https://doi.org/10.1158/1078−0432.Ccr−04−2236
9. Grainger S, Savory JG, Lohnes D (2010) Cdx2 regulates patterning of the intestinal epithelium. Dev Biol 339:155–165. https://doi.org/10.1016/j.ydbio. 2009. 12. 025
10. Silberg DG, Swain GP, Suh ER, Traber PG (2000) Cdx1 and cdx2 expression during intestinal development. Gastroenterology 119:961–971. https://doi.org/10. 1053/gast.2000.18142
11. Zhou Q, Toivola DM, Feng N, Greenberg HB, Franke WW, Omary MB (2003) Keratin 20 helps maintain intermediate filament organization in intestinal epithelia. Mol Biol Cell 14:2959–2971. https://doi.org/ 10.1091/mbc. e03− 02− 0059
12. Bae JM, Lee TH, Cho NY, Kim TY, Kang GH (2015) Loss of CDX2 expression is associated with poor prognosis in colorectal cancer patients. World J Gastroenterol 21:1457–1467. https://doi.org/ 10.3748/wjg. v21. i5. 1457
13. Dalerba P, Sahoo D, Paik S, Guo XQ, Yothers G, Song N, Wilcox−Fogel N, Forgo E, Rajendran PS, Miranda SP, Hisamori S, Hutchison J, Kalisky T, Qian DL, Wolmark N, Fisher GA, van de Rijn M, Clarke MF (2016) CDX2 as a prognostic biomarker in stage II and stage III colon cancer. New Engl J Med 374:211–222. https://doi.org/10.1056/ NEJMo a1506 597
14. Hansen TF, Kjaer−Frifeldt S, Eriksen AC, Lindebjerg J, Jensen LH, Sorensen FB, Jakobsen A (2018) Prognostic impact of CDX2 in stage II colon cancer: results from two nationwide cohorts. Br J Cancer 119:1367–1373. https://doi.org/10.1038/s41416−018−0285−5
15. Slik K, Turkki R, Carpen O, Kurki S, Korkeila E, Sundstrom J, Pellinen T (2019) CDX2 loss with microsatellite stable phenotype predicts poor clinical outcome in stage II colorectal carcinoma. Am J Surg Pathol 43:1473–1482. https://doi.org/10.1097/PAS.0000000000001356
16. Graule J, Uth K, Fischer E, Centeno I, Galvan JA, Eichmann M, Rau TT, Langer R, Dawson H, Nitsche U, Traeger P, Berger MD,

Schnuriger B, Hadrich M, Studer P, Inderbitzin D, Lugli A, Tschan MP, Zlobec I (2018) CDX2 in colorectal cancer is an independent prognostic factor and regulated by promoter methylation and histone deacetylation in tumors of the serrated pathway. Clin Epigenetics 10:120. https://doi.org/10.1186/s13148- 018- 0548-2
17. Kim JH, Rhee YY, Bae JM, Cho NY, Kang GH (2013) Loss of CDX2/CK20 expression is associated with poorly differentiated carcinoma, the CpG island methylator phenotype, and adverse prognosis in microsatellite-unstable colorectal cancer. Am J Surg Pathol 37:1532–1541. https://doi.org/10.1097/PAS.0b013e31829ab1c1
18. Berg KB, Schaeffer DF (2017) SATB2 as an immunohistochemical marker for colorectal adenocarcinoma: a concise review of benefits and pitfalls. Arch Pathol Lab Med 141:1428–1433. https://doi.org/10.5858/arpa.2016-0243-RS
19. Magnusson K, de Wit M, Brennan DJ, Johnson LB, McGee SF, Lundberg E, Naicker K, Klinger R, Kampf C, Asplund A, Wester K, Gry M, Bjartell A, Gallagher WM, Rexhepaj E, Kilpinen S, Kallioniemi OP, Belt E, Goos J, Meijer G, Birgisson H, Glimelius B, Borrebaeck CA, Navani S, Uhlen M, O'Connor DP, Jirstrom K, Ponten F (2011) SATB2 in combination with cytokeratin 20 identifies over 95% of all colorectal carcinomas. Am J Surg Pathol 35:937–948. https://doi.org/10.1097/PAS.0b013e31821c3dae
20. Dragomir A, de Wit M, Johansson C, Uhlen M, Ponten F (2014) The role of SATB2 as a diagnostic marker for tumors of colorectal origin: results of a pathology-based clinical prospective study. Am J Clin Pathol 141:630–638. https://doi.org/10.1309/AJCPWW2URZ9JKQJU
21. Dabir PD, Svanholm H, Christiansen JJ (2018) SATB2 is a supplementary immunohistochemical marker to CDX2 in the diagnosis of colorectal carcinoma metastasis in an unknown primary. APMIS 126:494–500. https://doi.org/10.1111/apm.12854
22. Eberhard J, Gaber A, Wangefjord S, Nodin B, Uhlen M, Ericson Lindquist K, Jirstrom K (2012) A cohort study of the prognostic and treatment predictive value of SATB2 expression in colorectal cancer.

Br J Cancer 106:931–938. https://doi.org/10.1038/bjc.2012. 34
23. Ma C, Olevian D, Miller C, Herbst C, Jayachandran P, Kozak MM, Chang DT, Pai RK (2019) SATB2 and CDX2 are prognostic biomarkers in DNA mismatch repair protein deficient colon cancer. Mod Pathol 32:1217–1231. https://doi.org/10.1038/s41379-019-0265-1
24. Ma C, Olevian DC, Lowenthal BM, Jayachandran P, Kozak MM, Chang DT, Pai RK (2018) Loss of SATB2 expression in colorectal carcinoma is associated with DNA mismatch repair protein deficiency and BRAF mutation. Am J Surg Pathol 42:1409–1417. https://doi.org/10.1097/PAS.0000000000001116
25. Baba Y, Nosho K, Shima K, Freed E, Irahara N, Philips J, Meyerhardt JA, Hornick JL, Shivdasani RA, Fuchs CS, Ogino S (2009) Relationship of CDX2 loss with molecular features and prognosis in colorectal cancer. Clin Cancer Res 15:4665–4673. https://doi.org/10.1158/1078-0432.CCR-09-0401
26. Dawson H, Koelzer VH, Lukesch AC, Mallaev M, Inderbitzin D, Lugli A, Zlobec I (2013) Loss of Cdx2 expression in primary tumors and lymph node metastases is specific for mismatch repair deficiency in colorectal cancer. Front Oncol 3:265. https://doi.org/10.3389/fonc.2013.00265
27. Dawson H, Galvan JA, Helbling M, Muller DE, Karamitopoulou E, Koelzer VH, Economou M, Hammer C, Lugli A, Zlobec I (2014) Possible role of Cdx2 in the serrated pathway of colorectal cancer characterized by BRAF mutation, high-level CpG Island methylator phenotype and mismatch repair-deficiency. Int J Cancer 134:2342–2351. https://doi.org/10.1002/ijc.28564
28. Boland CR, Thibodeau SN, Hamilton SR, Sidransky D, Eshleman JR, Burt RW, Meltzer SJ, Rodriguez-Bigas MA, Fodde R, Ranzani GN, Srivastava S (1998) A National Cancer Institute Workshop on Microsatellite Instability for cancer detection and familial predisposition: development of international criteria for the determination of microsatellite instability in colorectal cancer. Cancer Res 58:5248–5257
29. Lugli A, Kirsch R, Ajioka Y, Bosman F, Cathomas G, Dawson H,

El Zimaity H, Flejou JF, Hansen TP, Hartmann A, Kakar S, Langner C, Nagtegaal I, Puppa G, Riddell R, Ristimaki A, Sheahan K, Smyrk T, Sugihara K, Terris B, Ueno H, Vieth M, Zlobec I, Quirke P (2017) Recommendations for reporting tumor budding in colorectal cancer based on the International Tumor Budding Consensus Conference (ITBCC) 2016. Mod Pathol 30:1299-1311. https://doi.org/10.1038/modpathol.2017.46
30. Ueno H, Kajiwara Y, Shimazaki H, Shinto E, Hashiguchi Y, Nakanishi K, Maekawa K, Katsurada Y, Nakamura T, Mochizuki H, Yamamoto J, Hase K (2012) New criteria for histologic grading of colorectal cancer. Am J Surg Pathol 36:193-201. https://doi.org/10.1097/PAS.0b013e318235edee
31. Ueno H, Kanemitsu Y, Sekine S, Ishiguro M, Ito E, Hashiguchi Y, Kondo F, Shimazaki H, Kajiwara Y, Okamoto K, Mochizuki S, Tsujimoto H, Shinto E (2019) A Multicenter Study of the Prognostic Value of Desmoplastic Reaction Categorization in Stage II Colorectal Cancer. Am J Surg Pathol 43:1015-1022. https://doi.org/10.1097/PAS.0000000000001272
32. Ueno H, Hashiguchi Y, Shimazaki H, Shinto E, Kajiwara Y, Nakanishi K, Kato K, Maekawa K, Miyai K, Nakamura T, Yamamoto J, Hase K (2013) Objective criteria for crohn-like lymphoid reaction in colorectal cancer. Am J Clin Pathol 139:434-441. https://doi.org/10.1309/AJCPWHUEFTGBWKE4
33. Kim JH, Kim KJ, Bae JM, Rhee YY, Cho NY, Lee HS, Kang GH (2015) Comparative validation of assessment criteria for Crohn-like lymphoid reaction in colorectal carcinoma. J Clin Pathol 68:22-28. https://doi.org/10.1136/jclinpath-2014-202603
34. Lee JA, Yoo SY, Oh HJ, Jeong S, Cho NY, Kang GH, Kim JH (2021) Differential immune microenvironmental features of microsatellite-unstable colorectal cancers according to Fusobacterium nucleatum status. Cancer Immunol Immunother 70:47-59. https://doi.org/10.1007/s00262-020-02657-x
35. Oh HJ, Kim JH, Lee TH, Park HE, Bae JM, Lee HS, Kang GH (2017) Dominant high expression of wild-type HSP110 defines a poor prognostic subgroup of colorectal carcinomas with microsatellite instability: a whole-section immunohistochemical

analysis. APMIS 125:1076–1083. https://doi.org/10.1111/apm.12770
36. Bankhead P, Loughrey MB, Fernandez JA, Dombrowski Y, McArt DG, Dunne PD, McQuaid S, Gray RT, Murray LJ, Coleman HG, James JA, Salto–Tellez M, Hamilton PW (2017) QuPath: Open source software for digital pathology image analysis. Sci Rep 7:16878. https://doi.org/10.1038/s41598–017–17204–5
37. Loughrey MB, Bankhead P, Coleman HG, Hagan RS, Craig S, McCorry AMB, Gray RT, McQuaid S, Dunne PD, Hamilton PW, James JA, Salto–Tellez M (2018) Validation of the systematic scoring of immunohistochemically stained tumour tissue microarrays using QuPath digital image analysis. Histopathology 73:327–338. https://doi.org/10.1111/his.13516
38. Pages F, Mlecnik B, Marliot F, Bindea G, Ou FS, Bifulco C, Lugli A, Zlobec I, Rau TT, Berger MD, Nagtegaal ID, Vink–Borger E, Hartmann A, Geppert C, Kolwelter J, Merkel S, Grutzmann R, Van den Eynde M, Jouret–Mourin A, Kartheuser A, Leonard D, Remue C, Wang JY, Bavi P, Roehrl MHA, Ohashi PS, Nguyen LT, Han S, MacGregor HL, Hafezi–Bakhtiari S, Wouters BG, Masucci GV, Andersson EK, Zavadova E, Vocka M, Spacek J, Petruzelka L, Konopasek B, Dundr P, Skalova H, Nemejcova K, Botti G, Tatangelo F, Delrio P, Ciliberto G, Maio M, Laghi L, Grizzi F, Fredriksen T, Buttard B, Angelova M, Vasaturo A, Maby P, Church SE, Angell HK, Lafontaine L, Bruni D, El Sissy C, Haicheur N, Kirilovsky A, Berger A, Lagorce C, Meyers JP, Paustian C, Feng Z, Ballesteros–Merino C, Dijkstra J, van de Water C, van Lent–van Vliet S, Knijn N, Musina AM, Scripcariu DV, Popivanova B, Xu M, Fujita T, Hazama S, Suzuki N, Nagano H, Okuno K, Torigoe T, Sato N, Furuhata T, Takemasa I, Itoh K, Patel PS, Vora HH, Shah B, Patel JB, Rajvik KN, Pandya SJ, Shukla SN, Wang Y, Zhang G, Kawakami Y, Marincola FM, Ascierto PA, Sargent DJ, Fox BA, Galon J (2018) International validation of the consensus Immunoscore for the classification of colon cancer: a prognostic and accuracy study. Lancet 391:2128–2139. https://doi.org/10.1016/S0140–6736(18)30789–X

39. Taube JM, Galon J, Sholl LM, Rodig SJ, Cottrell TR, Giraldo NA, Baras AS, Patel SS, Anders RA, Rimm DL, Cimino-Mathews A (2018) Implications of the tumor immune microenvironment for staging and therapeutics. Mod Pathol 31:214-234. https://doi.org/10.1038/modpathol.2017.156
40. Bae JM, Kim JH, Oh HJ, Park HE, Lee TH, Cho NY, Kang GH (2017) Downregulation of acetyl-CoA synthetase 2 is a metabolic hallmark of tumor progression and aggressiveness in colorectal carcinoma. Mod Pathol 30:267-277. https://doi.org/10.1038/modpathol.2016.172
41. Guinney J, Dienstmann R, Wang X, de Reynies A, Schlicker A, Soneson C, Marisa L, Roepman P, Nyamundanda G, Angelino P, Bot BM, Morris JS, Simon IM, Gerster S, Fessler E, De Sousa EMF, Missiaglia E, Ramay H, Barras D, Homicsko K, Maru D, Manyam GC, Broom B, Boige V, Perez-Villamil B, Laderas T, Salazar R, Gray JW, Hanahan D, Tabernero J, Bernards R, Friend SH, Laurent-Puig P, Medema JP, Sadanandam A, Wessels L, Delorenzi M, Kopetz S, Vermeulen L, Tejpar S (2015) The consensus molecular subtypes of colorectal cancer. Nat Med 21:1350-1356. https://doi.org/10.1038/nm.3967
42. Kim JH, Kang GH (2014) Molecular and prognostic heterogeneity of microsatellite-unstable colorectal cancer. World J Gastroenterol 20:4230–4243. https://doi.org/10.3748/wjg.v20.i15.4230
43. Weisenberger DJ, Siegmund KD, Campan M, Young J, Long TI, Faasse MA, Kang GH, Widschwendter M, Weener D, Buchanan D, Koh H, Simms L, Barker M, Leggett B, Levine J, Kim M, French AJ, Thibodeau SN, Jass J, Haile R, Laird PW (2006) CpG island methylator phenotype underlies sporadic microsatellite instability and is tightly associated with BRAF mutation in colorectal cancer. Nat Genet 38:787–793. https://doi.org/10.1038/ng1834
44. Yan HHN, Lai JCW, Ho SL, Leung WK, Law WL, Lee JFY, Chan AKW, Tsui WY, Chan ASY, Lee BCH, Yue SSK, Man AHY, Clevers H, Yuen ST, Leung SY (2017) RNF43 germline and somatic mutation in serrated neoplasia pathway and its association with BRAF mutation. Gut 66:1645–1656. https://doi.org/10.1136/gutjnl- 2016-311849

45. Guinney J, Dienstmann R, Wang X, de Reynies A, Schlicker A, Soneson C, Marisa L, Roepman P, Nyamundanda G, Angelino P, Bot BM, Morris JS, Simon IM, Gerster S, Fessler E, De Sousa EMF, Missiaglia E, Ramay H, Barras D, Homicsko K, Maru D, Manyam GC, Broom B, Boige V, Perez-Villamil B, Laderas T, Salazar R, Gray JW, Hanahan D, Tabernero J, Bernards R, Friend SH, Laurent-Puig P, Medema JP, Sadanandam A, Wessels L, Delorenzi M, Kopetz S, Vermeulen L, Tejpar S (2015) The consensus molecular subtypes of colorectal cancer. Nat Med 21:1350–1356. https://doi.org/10.1038/nm.3967
46. Cancer Genome Atlas N (2012) Comprehensive molecular characterization of human colon and rectal cancer. Nature 487:330–337. https://doi.org/10.1038/nature11252
47. Kim JH, Kang GH (2020) Evolving pathologic concepts of serrated lesions of the colorectum. J Pathol Transl Med 54:276–289. https://doi.org/10.4132/jptm.2020.04.15
48. Kumar N, Tsai YH, Chen L, Zhou A, Banerjee KK, Saxena M, Huang S, Toke NH, Xing J, Shivdasani RA, Spence JR, Verzi MP (2019) The lineage-specific transcription factor CDX2 navigates dynamic chromatin to control distinct stages of intestine development. Development 146 https://doi.org/10.1242/dev.172189
49. Brocato J, Costa M (2015) SATB1 and 2 in colorectal cancer. Carcinogenesis 36:186–191. https://doi.org/10.1093/carcin/bgu322
50. Ehrlich M (2019) DNA hypermethylation in disease: mechanisms and clinical relevance. Epigenetics 14:1141–1163. https://doi.org/10.1080/15592294.2019.1638701
51. Xu M, Xu X, Pan B, Chen X, Lin K, Zeng K, Liu X, Xu T, Sun L, Qin J, He B, Pan Y, Sun H, Wang S (2019) LncRNA SATB2-AS1 inhibits tumor metastasis and affects the tumor immune cell microenvironment in colorectal cancer by regulating SATB2. Mol Cancer 18:135. https://doi.org/10.1186/s12943-019-1063-6
52. Wang YQ, Jiang DM, Hu SS, Zhao L, Wang L, Yang MH, Ai ML, Jiang HJ, Han Y, Ding YQ, Wang S (2019) SATB2-AS1 suppresses colorectal carcinoma aggressiveness by inhibiting SATB2-dependent snail transcription and epithelial-mesenchymal transition.

Cancer Res 79:3542–3556. https://doi.org/10.1158/0008-5472.CAN-18-2900
53. Chen QY, Des Marais T, Costa M (2019) Deregulation of SATB2 in carcinogenesis with emphasis on miRNA-mediated control. Carcinogenesis 40:393–402. https://doi.org/10.1093/carcin/bgz020
54. Verzi MP, Shin H, He HH, Sulahian R, Meyer CA, Montgomery RK, Fleet JC, Brown M, Liu XS, Shivdasani RA (2010) Differentiation-specific histone modifications reveal dynamic chromatin interactions and partners for the intestinal transcription factor CDX2. Dev Cell 19:713–726. https://doi.org/10.1016/j.devcel.
55. Kawai H, Tomii K, Toyooka S, Yano M, Murakami M, Tsukuda K, Shimizu N (2005) Promoter methylation downregulates CDX2 expression in colorectal carcinomas. Oncol Rep 13:547–551
56. Liao W, Overman MJ, Boutin AT, Shang X, Zhao D, Dey P, Li J, Wang G, Lan Z, Li J, Tang M, Jiang S, Ma X, Chen P, Katkhuda R, Korphaisarn K, Chakravarti D, Chang A, Spring DJ, Chang Q, Zhang J, Maru DM, Maeda DY, Zebala JA, Kopetz S, Wang YA, DePinho RA (2019) KRAS-IRF2 axis drives immune suppression and immune therapy resistance in colorectal cancer. Cancer Cell 35(559–572):e557. https://doi.org/10.1016/j.ccell.2019.02.008
57. Lal N, White BS, Goussous G, Pickles O, Mason MJ, Beggs AD, Taniere P, Willcox BE, Guinney J, Middleton GW (2018) KRAS mutation and consensus molecular subtypes 2 and 3 are independently associated with reduced immune infiltration and reactivity in colorectal cancer. Clin Cancer Res 24:224–233. https://doi.org/10.1158/1078-0432.CCR-17-1090

.

초록

미골부유형 호메오박스2 (CDX2), 특수 AT 서열 결합 단백2 (SATB2), 그리고 케라틴 20(KRT20)은 면역조직화학 연구에서 장 상피 특이적 표지자로 자주 사용된다. 하지만, 대장암의 일부에서는 이들 표지자를 발현하지 않는다. 이번 연구에서 암유전체지도 데이터를 분석하여 390개의 대장암에서 CDX2, SATB2 그리고 KRT20 유전자의 분자적 상관 관계를 조사하였다. 3가지 유전자 각각의 감소된 mRNA 발현은 일반적으로 높은 미세부수체 불안정성 (MSI-H), CpG island methylator phenotype-high (CIMP-H), BRAF/RNF43의 돌연변이, 공통 분자 아형 1 및 높은 종양 변이 부담과 상관관계가 있는 것으로 나타났다. CDX2 또는 SATB2의 하향조절은 MSI-H와 CIMP-H 모두에 의존하는 반면, KRT20의 하향조절은 CIMP-H보다 MSI-H에 더 의존적이었다. 다음으로 우리는 436개의 원발성 대장암에서 CDX2, SATB2 및 KRT20의 면역조직화학적 발현을 평가했다. RNA 수준의 발현과 대조적으로, CDX2 및 SATB2의 감소된 단백질 발현은 MSI-H보다 CIMP-H에 더 의존적이었다. 그러나, RNA 수준 발현과 일치하게, KRT20의 감소된 단백질 발현은 CIMP-H보다 MSI-H에 더 의존적이었다. CIMP-H 및 림프관 침범은 MSI 상태에 관계없이 대장암에서 CDX2 및 SATB2의 발현 손실과 일관되게 연관되었다. 3가지 표지자가 동시에 손실된 경우는 MLH1이 메틸화된 MSI-H/CIMP-H 대장암에서만 독점적으로 발견되었다. 결론적으로, MSI-H 및 CIMP-H는 결장암에서 감소된 CDX2/SATB2/KRT20 발현의 주요 공통 상관관계이지만, 각 표지자의 손실과 관련된 특성들은 대장암에서 다르게 나타났다.